

This article was downloaded by:

On: 30 January 2011

Access details: *Access Details: Free Access*

Publisher *Taylor & Francis*

Informa Ltd Registered in England and Wales Registered Number: 1072954 Registered office: Mortimer House, 37-41 Mortimer Street, London W1T 3JH, UK



Separation & Purification Reviews

Publication details, including instructions for authors and subscription information:

<http://www.informaworld.com/smpp/title~content=t713597294>

Progress in Parametric Pumping

Richard G. Rice^a

^a Rice University of Queensland, St. Lucia, Queensland, Australia

To cite this Article Rice, Richard G.(1976) 'Progress in Parametric Pumping', *Separation & Purification Reviews*, 5: 1, 139 — 188

To link to this Article: DOI: 10.1080/03602547608066050

URL: <http://dx.doi.org/10.1080/03602547608066050>

PLEASE SCROLL DOWN FOR ARTICLE

Full terms and conditions of use: <http://www.informaworld.com/terms-and-conditions-of-access.pdf>

This article may be used for research, teaching and private study purposes. Any substantial or systematic reproduction, re-distribution, re-selling, loan or sub-licensing, systematic supply or distribution in any form to anyone is expressly forbidden.

The publisher does not give any warranty express or implied or make any representation that the contents will be complete or accurate or up to date. The accuracy of any instructions, formulae and drug doses should be independently verified with primary sources. The publisher shall not be liable for any loss, actions, claims, proceedings, demand or costs or damages whatsoever or howsoever caused arising directly or indirectly in connection with or arising out of the use of this material.

PROGRESS IN PARAMETRIC PUMPING

Richard G. Rice
University of Queensland
St. Lucia, Queensland, Australia

Introduction

Parametric pumping is the name given to a novel separation device developed by Richard Wilhelm and co-workers^(1,2,3). The principle of operation depends on an immobile phase (e.g. adsorbent) to alternately retard and release selected species. This action coupled with a synchronous periodic fluid flow causes the selectively adsorbed species to be literally *pumped* from one region to another. In the successful experiments^(2,3), a single packed column was used with reservoirs attached to each end. A water jacket surrounding the bed was heated or cooled synchronously with periodic fluid motion. Figure 1 outlines the principle of operation. Essentially, the process operates in a "bucket-brigade" fashion. If one follows the travels of a single solute (see Figure 1) in a non-adsorbable solvent we see that during downflow the column is cooled thus retarding (adsorption step) the solute, allowing the solvent to move unimpeded. When the flow direction changes to an upward motion, the column is heated, releasing (desorption step) the solute and sweeping it upward. Repeating this cycle, one sees that the solute hops in bucket-brigade fashion toward the upper reservoir until it is eventually captured. Separation factors (i.e., ratio of rich to lean reservoir composition) as large as $10^5:1$ have been reported^(2,3). The fundamental

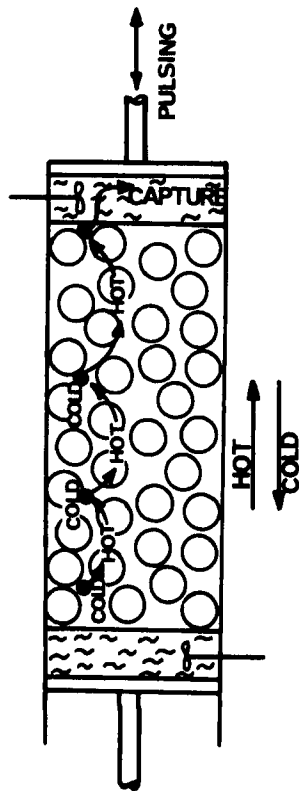


FIGURE 1a

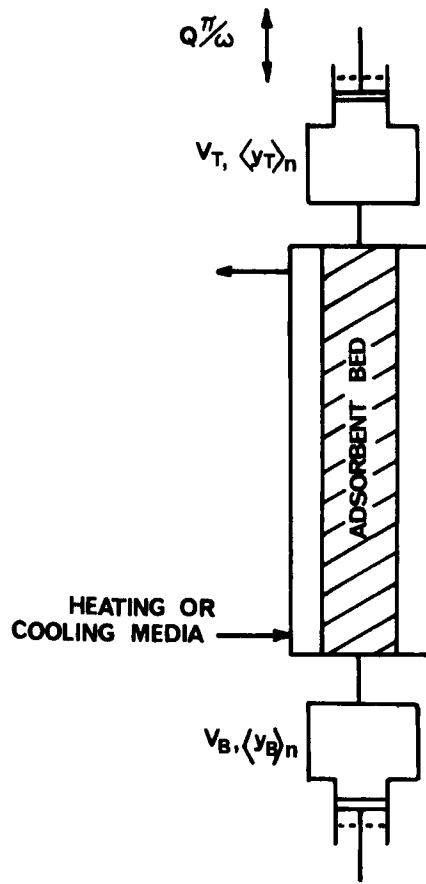


FIGURE 1b

FIGURE 1

(a) Schematic representation of the journey of a solute molecule
 (b) Schematic of a closed direct-thermal-mode parapump

driving force for separation is the adsorbed phase concentration difference at the two operating temperatures. This difference depends on the shape of the isotherms as shown in Figure 2. The method of operation thus outlined has been called the direct-

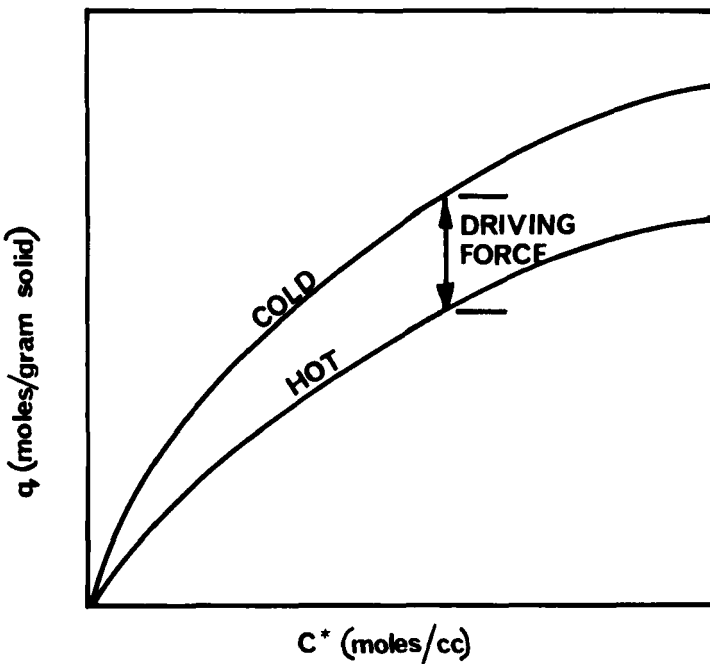


FIGURE 2

Typical adsorption isotherms for successful parapump operation

thermal-mode⁽³⁾. The principle of operation is not limited to a thermally induced retardation-release step, and in fact Thompson and Bass^(4,5) recently used electrode potential to induce retardation. Furthermore, in a short note Lee and Kirwan⁽⁶⁾ outlined results whereby a porous carbon electrode sustained markedly different adsorption levels of biosubstances (glucoamylase) with increases in applied voltage. In one of his earlier papers⁽³⁾, Wilhelm suggests a variety of driving potentials may be used, including electrical, pressure, magnetic, and chemical (e.g., pH). Obviously, any potential which can be effectively tuned so as to induce a retard-release mechanism could be used in designing a parametric pump. The trick is to discover a retardation-release mechanism which is selective, that is, only the desired species

is pumped, while other species remain stagnant or move in the opposite direction (e.g., abnormal isotherm). By way of introduction, it should be noted that the parametric pumping technique is not limited to closed (batch) systems, but can be operated in a continuous and semi-continuous mode. Recent work on such open systems will also be treated in another section.

A rather up-to-date (to Oct. 1973) bibliography of published papers on cyclic processes has recently appeared (Wankat⁽⁷⁾). The current progress report will attempt to bring together the original theories and subsequent corrections (including a careful explanation of the mathematics) in a manner which is tractable to a novice in the field. It is important that new or novel separation techniques reach as wide an audience as possible, especially those practitioners outside the field of Chemical Engineering. Applications of parametric pumping range from isotope enrichment to enzyme separation, and possible future applications toward a compact artificial kidney. The technique and its future are truly multi-disciplinary.

Closed Systems

In this section, the early work on closed (batch) systems is briefly reviewed. The principal types of thermal stimulation, that is the Direct-Thermal-Mode (DTM) and the Recuperative Mode (RM), are treated separately. In addition, the recent work of Thompson and Bass^(4,5) using electrical stimulation will be considered. By way of introduction to the underlying principle of parapumping, the pioneering *equilibrium theory* of Pigford, Baker and Blum⁽⁸⁾ will be treated in detail. The section is concluded with a discussion of the problem of predicting *ultimate separation* with special attention to design considerations.

The Equilibrium Theory of Direct-Thermal-Mode (DTM)

To appreciate the important idealizations of Pigford, et al.'s *Equilibrium Theory*, we write the complete chromatographic equations for a flowing solution with single adsorbate.

The solute balance on combined fluid and solid phases within the column is:

$$\begin{aligned} \frac{\partial c}{\partial t} + \frac{(1-\varepsilon_b)}{\varepsilon_b} \varepsilon_p \frac{\partial c^*}{\partial t} + \rho_s \frac{(1-\varepsilon_b)(1-\varepsilon_p)}{b \varepsilon_b} \frac{\partial q}{\partial t} + v \frac{\partial c}{\partial z} \\ = E \frac{\partial^2 c}{\partial z^2} + D \frac{1}{r} \frac{\partial}{\partial r} r \frac{\partial c}{\partial r} \end{aligned} \quad (1)$$

The energy balance on the flowing phase is:

$$\frac{\partial T}{\partial t} + v \frac{\partial T}{\partial z} = E \frac{\partial^2 T}{\partial z^2} + \alpha \frac{1}{r} \frac{\partial}{\partial r} r \frac{\partial T}{\partial r} \quad (2)$$

The solute balance on the solid phase, neglecting pore diffusion, is:

$$\frac{\partial q}{\partial t} + \frac{\varepsilon_p}{\rho_s(1-\varepsilon_p)} \frac{\partial c^*}{\partial t} = \frac{k_m a_p}{\rho_s(1-\varepsilon_p)(1-\varepsilon_b)} (c - c^*) \quad (3)$$

or, including pore diffusion

$$\frac{\partial c^*}{\partial t} + \rho_s \left(\frac{1-\varepsilon_p}{\varepsilon_p} \right) \frac{\partial q}{\partial t} = D_p \frac{1}{r_p^2} \frac{\partial}{\partial r_p} r_p^2 \frac{\partial c^*}{\partial r_p} . \quad (4)$$

which requires a boundary condition reflecting film resistance at the flowing fluid-solid interface

$$- D_p \frac{\partial c^*}{\partial r_p} = k_m (c - c^*) \quad (4.1)$$

Finally, the energy balance on the solid phase is (neglecting thermal diffusion effects inside the particle):

$$\frac{\partial T_s}{\partial t} = \frac{h_p a_h}{[\rho_s c_s (1-\varepsilon_p) + \rho_f c_f \varepsilon_p]} (T - T_s) \quad (5)$$

$$+ \frac{(1-\varepsilon_p) \rho_s \Delta H_{ads}}{[\rho_s c_s (1-\varepsilon_p) + \rho_f c_f \varepsilon_p]} \frac{\partial q}{\partial t}$$

In addition, a specific form for the periodicity of velocity and wall or jacket temperature must be stated, along with the specific type of adsorption equilibrium relationship obtaining, i.e. .

$$q = f(T, c^*) \quad (6)$$

Finally, external equations describing mixing and hold-up in the respective reservoirs must be written.

The type of model used by Wilhelm and co-workers for computer explorations included a single dissipative effect, giving a combined solute balance of:

$$\epsilon_b \rho_f \frac{\partial y}{\partial t} + \bar{\rho}_s (1-\epsilon_b) \frac{\partial x}{\partial t} + \rho_f v \frac{\partial y}{\partial z} = 0 \quad (7)$$

with a rate expression

$$\bar{\rho}_s (1-\epsilon_b) \frac{\partial x}{\partial t} = k_m a_p (y - y^*) \rho_f \quad (8)$$

where $\bar{\rho}_s$ is bulk solids density hence solids composition (x) includes adsorbed as well as pore fluid. By comparison with the complete transport equations given earlier it is easy to deduce the dissipative effects which are ignored in Wilhelm's model. In these simplified equations, the solid composition includes both adsorbed and pore fluid.

Pigford, et al.⁽⁸⁾ noticed that despite the large differences in composition at the ends of the packed column, the local composition differences (c and c^*) calculated by Wilhelm et al.⁽³⁾ via computer simulation of equations (7) and (8) were quite small. This important observation led Pigford to assume perfect local equilibrium ($k_m \rightarrow \infty$) between solid and fluid phases, considerably simplifying the mathematics.

Pigford thus proposed to explore the predictions of an equilibrium situation using equation (7) as the primary transport equation coupled with a linear equilibrium relationship taken as

$$x = M(t) y \quad (9)$$

where M is the equilibrium constant which depends on bed temperature. Inserting (9) into (7) there results,

$$\epsilon_b \rho_f \frac{\partial y}{\partial t} + \epsilon_b \rho_f v \frac{\partial y}{\partial z} + (1-\epsilon_b) \bar{\rho}_s [M \frac{\partial y}{\partial t} + \frac{dM}{dT} \frac{\partial T}{\partial t} y] = 0 \quad (10)$$

Combining the equilibrium constant with the column hold-up terms, this equation is rearranged to read

$$(1+m) \frac{\partial y}{\partial t} + v \frac{\partial y}{\partial z} = - \frac{\partial T}{\partial t} \frac{dm}{dT} \cdot y \quad (11)$$

where

$$m(T) = \bar{\rho}_s (1-\epsilon_b) M(T) / \rho_f \epsilon_b \quad . \quad (12)$$

Equation (11) can be solved by the method of characteristics; or very simply, one can see that the total differential of $y(z, t)$ is written

$$\frac{dy}{dt} = \frac{\partial y}{\partial z} \frac{dz}{dt} + \frac{\partial y}{\partial t} \quad (13)$$

Comparing this with equation (11), one deduces

$$\frac{dy}{dt} = - \frac{dm}{dt} \cdot y / (1+m) \quad (14)$$

and

$$\frac{v}{1+m} = \frac{dz}{dt} \quad (15)$$

provided temperature is an undistributed variable, i.e., $T(t)$. In the "direct mode" described by Wilhelm, Rice, Rolke and Sweed,⁽³⁾ fluid velocity is either upward or downward but always at a constant speed, v_0 , and hence can be represented by a square wave function

$$v = v_0 \operatorname{sq}(\omega t) \quad . \quad (16)$$

The synchronous applied temperature (assuming the bed responds instantaneously) produces an in-phase square wave change in equilibrium constant, which can be represented by

$$m = m_0 - a \operatorname{sq}(\omega t) \quad (17)$$

where "a" denotes the change in m taken around the mean value, m_0 . The negative sign reflects the case of normal isotherm behavior such that heating (upflow) produces a reduction in solid composition while cooling (downflow) increases solids composition. Inserting these periodic functions in the ordinary differential equations, (14) and (15) gives

$$\frac{dz}{dt} = \frac{v_0 \operatorname{sq}(wt)}{1+m_0 - a \operatorname{sq}(wt)} = \frac{u_0 \operatorname{sq}(wt)}{1-b \operatorname{sq}(wt)} \quad (18)$$

and

$$\frac{dy}{y} = \frac{d(m_0 - a \operatorname{sq}(wt))}{1+m_0 - a \operatorname{sq}(wt)} = - \frac{d(1-b \operatorname{sq}(wt))}{1-b \operatorname{sq}(wt)} \quad (19)$$

where the important parameter $b = a/1+m_0$ is defined.

The latter equation shows that during a half-cycle

$$y(1-b \operatorname{sq}(wt)) = \text{constant} \quad (20)$$

The trajectory (characteristic) followed by the fluid composition wave during a half-cycle is obtained by integrating eqn. (18) giving

$$\begin{aligned} z &= \frac{u_0}{1-b} t + \text{constant, hot upflow} \\ z &= \frac{-u_0}{1+b} t + \text{constant, cold downflow} \end{aligned} \quad (21)$$

The term u_0 represents the velocity of propagation of composition waves moving through the packing at the mean temperature and is given by:

$$u_0 = v_0 / 1+m_0 \quad (22)$$

which is always smaller than the fluid (solvent) velocity, v_0 . In the foregoing development, complete displacement of reservoirs is assumed and furthermore, reservoirs are taken to be perfectly mixed.

The trajectories followed by the concentration waves are straight lines with slopes $u_0/1-b$ during hot upflow and $-u_0/1+b$ during cold downflow. Along a characteristic path composed of connecting straight-line segments, the product $y(z,t)[1-b \operatorname{sq}(wt)]$ is constant, thus $y(z,t)$ undergoes a change in values proportional to the ratio $(1+b)/(1-b)$ when the characteristic trajectory passes from a cold region into a hot one, and the inverse of this in passing from hot to cold. Along each of the straight segments of a characteristic line, equation (20) shows that $y(z,t)$ is constant.

As Pigford, et al. noted, the problem of constructing a solution is reduced to the geometrical problem of locating the characteristics in the z versus t plane and counting the number of changes in slope which each characteristic experiences.

It is useful at this point to write expressions for the distance the concentration wave moves during one half-cycle, thus for the hot upflow:

$$L_H = \frac{u_H \pi}{(1-b) \omega} \quad (23)$$

and for cold downflow the penetration distance is:

$$L_c = \frac{u_c \pi}{(1+b) \omega} \quad (24)$$

For batch systems with equal displacements per half-cycle, $u_c = u_H = u_0$. One sees that if the column is sufficiently short, or u_0 is large enough, it would be possible for solute to leave one reservoir and pass through the column into the other reservoir without enrichment and thereby decrease the separation effect. To avoid this destructive situation, it is necessary to insure that

$$L_H < h \quad (25)$$

where h denotes the column height. This is the basis for the construction in Figure 3 after Pigford, et al.⁽⁸⁾ and Chen and Hill⁽⁹⁾.

The method of operation in Wilhelm's original experiments (and used as the basis for the Equilibrium Theory) was such that the volume of fluid displaced alternately from the end reservoirs was equal to the interstitial hold-up in the column, hence

$$v_0 \pi / \omega = h \quad (26)$$

or rewriting

$$\frac{u_0 \pi / \omega}{1-b} = \frac{h}{(1-b)(1+m_0)} = L_H \quad (27)$$

which shows that $L_H < h$ if $(1-b)(1+m_0) > 1$. However, since $b = a/1+m_0$ and eqn. (17) shows that $a < m_0$ hence always $(1-b)(1+m_0) = 1+m_0 - a > 1$ and $L_H < h$ as required.

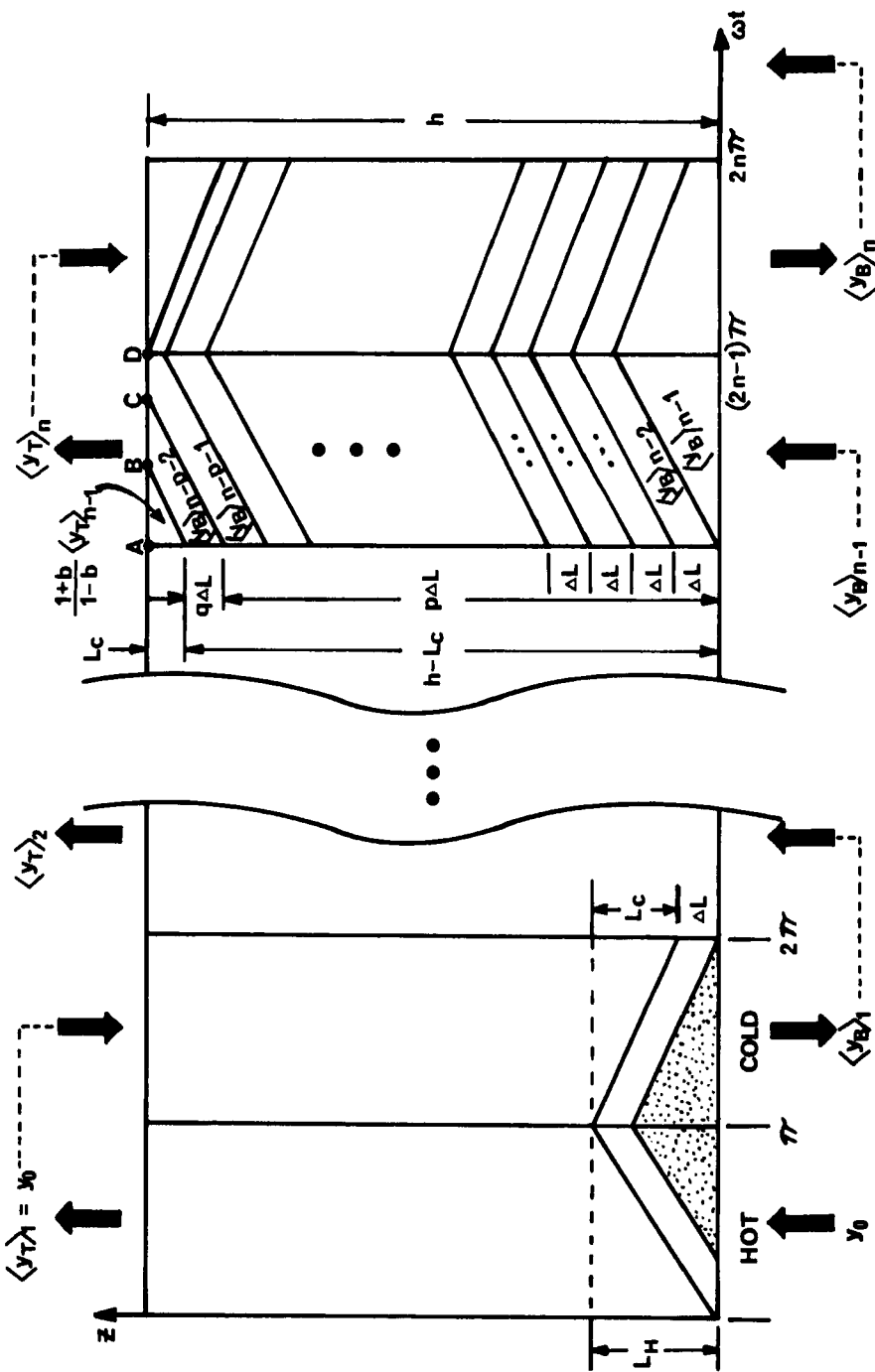


FIGURE 3. Characteristics for batch operation.

Because of its importance in explaining the origin of separation in parapumps, we continue with Pigford's development of the Equilibrium Theory. It should be noted very early in the discussion that Aris⁽¹⁰⁾ found that Pigford treated a special case, and a more general theory evolved which will be presented shortly.

Referring to Figure 3, the operation of the parapump begins with the column filled with fluid of concentration y_0 in equilibrium with the solid at the higher system temperature. The bottom reservoir is filled with fluid of this same composition. Reservoir displacement volume is equivalent to the interstitial hold-up in the column. The upper reservoir is initially empty. The initial motion is upward while the column is hot. The mixed mean composition of the fluid displaced to the top of the column during the hot n^{th} half-cycle is denoted by $\langle y_T \rangle_n$. The well-mixed feature of the slug of fluid existing in a reservoir at the end of a half-cycle is fundamental to the Equilibrium Theory, since Thompson and Bowen⁽¹¹⁾ theoretically predicted that reservoir mixing actually diminishes enrichment, contrary to the inference of Sweed and Wilhelm⁽¹²⁾.

To find the mixed-mean composition $\langle y_T \rangle_1$ at the end of the first hot half-cycle, it is necessary to find the source of the characteristic trajectory which crosses the line $z = h$. The number of concentration changes owing to temperature changes must be accounted for in order to determine the enrichment. During the first hot half-cycle, $0 < \omega t < \pi$, the characteristic lines (see eq. 21) which cross $z = h$ all begin along the line $t = 0$, where $y(z, t) = y_0$. The concentration remains constant along each of the characteristic lines (c.f. eq. 20) proceeding diagonally toward the line $z = h$ leading to a top product concentration of

$$\langle y_T \rangle_1 = y_0 \quad (28)$$

this composition is now injected as feed during the cold part of the first cycle.

During the cold downflow period of the first cycle, $\pi < \omega t < 2\pi$, all the characteristic lines crossing $z = 0$ (entering the

lower reservoir) actually originated from $z = 0$ during the preceding hot half-cycle. This occurs as a consequence of the difference in concentration wave penetration distance ($L_H > L_C$), since the magnitude of the characteristic slope for the hot cycle is greater than the slope for the cold cycle (eq. 21). The concentration $y(0,t) = y_0$ is preserved until $wt = \pi$ where a change in temperature takes place. The concentration then changes to $y_0 \left(\frac{1-b}{1+b}\right)$ as a consequence of eq. (20). This continues to the bottom of the column so that

$$\langle y_B \rangle_1 = y_0 \left(\frac{1-b}{1+b}\right) \quad (29)$$

This diminished concentration comprises the feed for the hot part of the second cycle. It is easy to see that the future of lower reservoir concentration proceeds as

$$\langle y_B \rangle_n = y_0 \left(\frac{1-b}{1+b}\right)^n = y_0 (\Gamma)^n \quad (30)$$

where we introduce the rate factor (eigenvalue) $\Gamma = 1-b/1+b$. However the future of upper reservoir concentrations presents difficulties associated with the way waves (bands) of different composition enter the upper reservoir. That is, we are concerned with the number of cycles for a concentration wave to move from bottom to top, as well as the weighting to be associated with waves of different history in calculating a mixed-mean reservoir composition.

Aris⁽¹⁰⁾ generalized the special case treated by Pigford et al. by letting wave velocity u_0 depend on the equilibrium parameter b as

$$\frac{\omega h}{\pi u_0} = \frac{1 + (2p + 2q - 1)b}{(1-b)(1+b)} \quad (31)$$

Aris noted that Pigford's analysis was not general since a characteristic from the origin would arrive at the exit of the bed after a time of exactly $3\pi/\omega$, hence for this special case

$$\frac{\omega h}{\pi u_0} = \frac{1 + 3b}{(1-b)(1+b)} \quad (32)$$

which allows only two types of intersection at $z = h$.

On first glance, the physical meaning of the parameters p and q seems obscure and little guidance was provided in the original paper. However, Chen and Hill⁽⁹⁾ later rearranged this expression to read

$$p + q = (h - L_c) / (L_H - L_c) \quad (33)$$

which lends itself to a simple geometrical interpretation as shown in Figure 3. In the remainder of the derivation, we assume $L_c < L_H < h$, this prevents solute mixing between reservoirs (Region I operation according to the definitions by Chen and Hill). The penetration distance term $(L_H - L_c)$ is the net upward movement per cycle of a slug of enriched material, hence "p" is the number (integer) of complete cycles required to transport a portion (any portion) of this slug from the bottom to the top reservoir. From the geometry, q ($0 \leq q < 1$) is obviously the fraction of this same slug which did not penetrate into the upper reservoir at the end of the p^{th} hot cycle. At the end of the $(p+1)^{\text{th}}$ hot cycle all of the original slug would have been assimilated into the well mixed reservoir. Chen and Hill⁽⁹⁾ state that when $q = 0$ only two composition waves move into the upper reservoir, but when $q > 0$ three compositions emerge. It was also stated that three is the maximum number of concentrations which can emerge, but the proof of this generalization has yet to be published.

Returning to the second cycle analysis of the upper reservoir, it is seen in Figure 3 that three kinds of concentration waves (characteristics) cross the upper boundary at $z = h$. Those intersecting along AB have come from the upper reservoir during the previous cold-half-cycle and have the composition $\langle y_T \rangle_2 = \frac{1+b}{1-b} y_0$, since $\langle y_T \rangle_1 = y_0$. The enrichment comes from the fact that composition waves entering along AB arise from characteristics which

have crossed the vertical line at $wt = 2\pi$, where there is a favorable temperature change.

For this second cycle, characteristics crossing both the regions BC and CD have originated from the initial contents of the column and have undergone compensating temperature changes before entering the top reservoir. Hence along both BC and CD the wave composition is simply y_0 .

Continuing in this way, one sees that after the system sustains $(p+1)$ cycles the initial contents no longer affects the solution of the problem if $q > 0$ (or p cycles if $q = 0$, see Pigford et al.). This reasoning is important in setting the proper initial condition on the general n^{th} cycle finite-difference equation, the development of which follows.

To find the mean composition of the upper reservoir, one simply sums the compositions of the enriched bands, each multiplied by a suitable weighting factor. Figure 4 shows contributions for the general n^{th} cycle; the upper reservoir receives bands of material from $\langle y_T \rangle_{n-1}$, $\langle y_B \rangle_{n-p-1}$ and $\langle y_B \rangle_{n-p-2}$. Before entering the top reservoir $\langle y_T \rangle_{n-1}$ suffers one temperature change, hence its injection concentration is $\langle y_T \rangle_{n-1} \left(\frac{1+b}{1-b}\right)$. The remaining composition waves undergo a sequence of compensatory changes hence retain their composition. The weighting associated with each composition wave is calculated from the fraction of the half-cycle time during which the particular wave is injected, or from the geometry the weights are

$$\begin{aligned} AB/AD &= L_c/L_H; BC/AD = q(1-L_c/L_H); CD/AD \\ &= (1-q)(1-L_c/L_H) \end{aligned} \quad (34)$$

Since equal displacements are used, $L_c/L_H = \frac{1-b}{1+b}$ for this particular case. From this, one sees there are only two contributions if $q = 0$ (which is the special case treated by Pigford). Summing up the weighted contributions to the top reservoir at the end of the n^{th} hot-half-cycle, there results for $n > p+1$

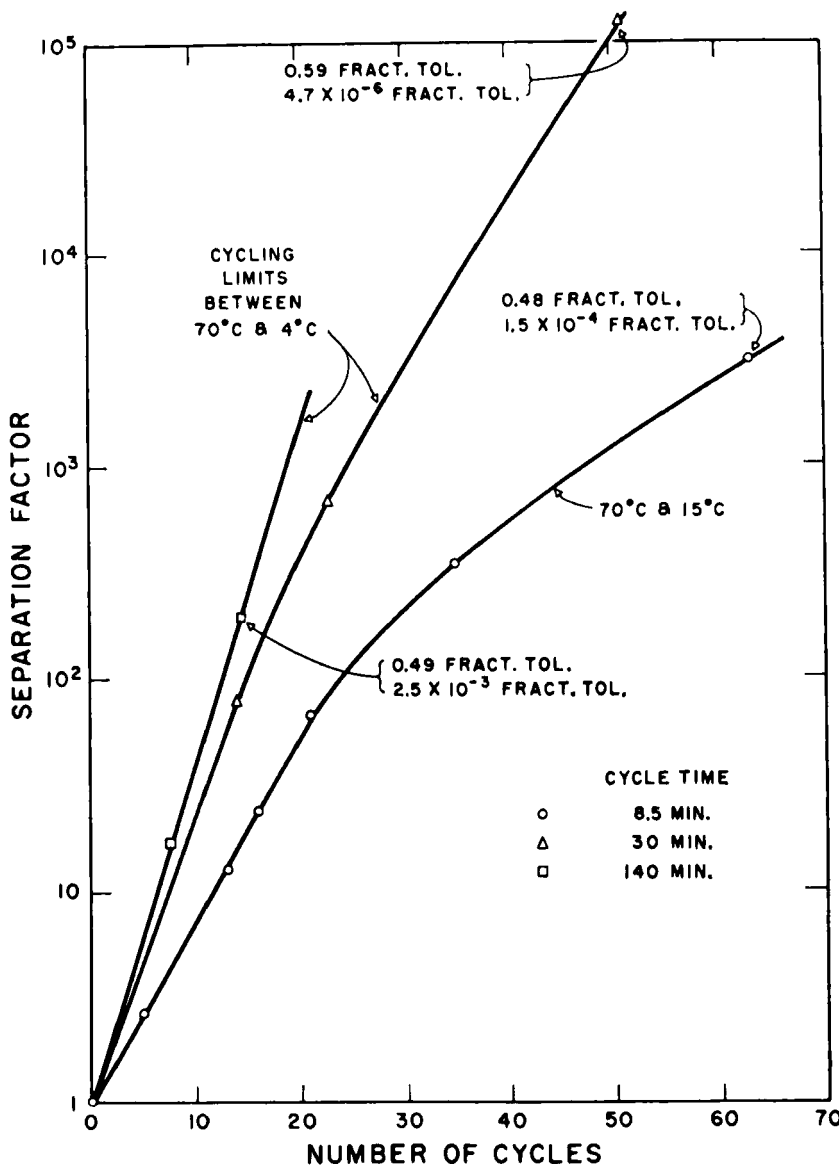


FIGURE 4

Separation factor versus cycle number from the original experiments of Wilhelm et al (3) (Reprinted with permission from Ind. Eng. Chem. Fundam.)

$$\begin{aligned} \langle y_T \rangle_n &= \langle y_T \rangle_{n-1} \left(\frac{1+b}{1-b} \right) \times \frac{AB}{AD} + \langle y_B \rangle_{n-p-2} \times \frac{BC}{AD} \\ &+ \langle y_B \rangle_{n-p-1} \times \frac{CD}{AD} \end{aligned} \quad (35)$$

Hence, the finite difference relationship describing enrichment as a function of cycle number is, after using eq. (30):

$$\begin{aligned} \langle y_T \rangle_n - \langle y_T \rangle_{n-1} &= y_0 \frac{q}{1+b} \left(\frac{1-b}{1+b} \right)^{n-p-2} \\ &+ y_0 \frac{(1-q)2b}{1+b} \left(\frac{1-b}{1+b} \right)^{n-p-1} \end{aligned} \quad (36)$$

The complementary solution to this linear finite difference equation is a simple constant which can be determined from a suitable initial condition. Equation (35) is valid for $n < p+1$ provided all bottom compositions $\langle y_B \rangle_n$ are replaced with y_0 when the indices are zero or negative. Thus we have for $n < p+1$

$$\begin{aligned} \langle y_T \rangle_n &= \langle y_T \rangle_{n-1} + \frac{q}{1+b} y_0 + \frac{(1-q)2b}{1+b} y_0 \\ &= \langle y_T \rangle_{n-1} + \frac{2b}{1+b} y_0 \end{aligned} \quad (37)$$

which is independent of q . This relationship provides the means for obtaining the initial condition for equation (35). The solution to eq. (37) for the case p when $n < p+1$ is:

$$\langle y_T \rangle_n = B + y_0 \frac{2b}{1+b} n \quad (38)$$

where the constant B is determined from the condition $\langle y_T \rangle_1 = y_0$, giving

$$\frac{\langle y_T \rangle_n}{y_0} = \left(1 + \frac{2b}{1+b} (n-1) \right) \quad (39)$$

When this solution is coupled to the solution of eq. (36) at $n = p+1$ (or $n=p$, if $q=0$), the initial condition for eq. (36) is established. The general solution to eq. (36) takes the form for $n > p+1$

$$\langle y_T \rangle_n = A + \frac{2by_0}{1+b} \frac{\Gamma}{\Gamma - \Gamma} \{ qr^{n-p-2} + (1-q)r^{n-p-1} \} \quad (40)$$

where the eigenvalue is $\gamma = (1-b)/(1+b)$. Coupling eqs. (39) and (40) at $n = p+1$ allows the arbitrary constant to be determined, giving the complete solution for $n \geq p+1$ (finite q):

$$\frac{\langle y_T \rangle_n}{y_0} = [1+q + \frac{2b}{1+b} p + (\frac{1-b}{1+b})(1-q)] - (\frac{1-b}{1+b})^{n-p} [q(\frac{1+b}{1-b}) + (1-q)] \quad (41)$$

If $q=0$, the coupling takes place at $n=p$, since the initial column contents would not affect the reservoir compositions after only p cycles. Under these conditions, the following solution for $n \geq p$, $q=0$ results:

$$\frac{\langle y_T \rangle_n}{y_0} = 2 + \frac{2b}{1+b}(p-1) - (\frac{1-b}{1+b})^{n-p} \quad (42)$$

which agrees with the solution of Pigford et al.⁽⁸⁾ where for $q=0$, $p=2$, it was shown:

$$\frac{\langle y_T \rangle_n}{y_0} = 2 + \frac{2b}{1+b} - (\frac{1-b}{1+b})^{n-2} .$$

The general solution ($q>0$) represented by eq. (41) neither agrees with Aris⁽¹⁰⁾ nor Chen and Hill⁽⁹⁾. Aris⁽¹⁰⁾ did not indicate how he coupled his solutions, but even so, there is an inconsistency in his results. The Chen and Hill⁽¹⁰⁾ solution does not account for the fact that when no dead volume exists, the upstroke feed is $\langle y_B \rangle_{n-1}$, not $\langle y_B \rangle_n$. When this is accounted for, their solutions agree with the above result.

A separation factor can be defined for the general case ($q>0$) as $\langle y_T \rangle_n / \langle y_B \rangle_n$ giving for $n \geq p+1$

$$\alpha_n = [1+q + \frac{2b}{1+b} p + (\frac{1-b}{1+b})(1-q)](\frac{1+b}{1-b})^n - [q(\frac{1+b}{1-b}) + (1-q)](\frac{1+b}{1-b})^p \quad (43)$$

and for $n \leq p+1$, the separation factor is

$$\alpha_n = (1 + \frac{2b}{1+b}(n-1))(\frac{1+b}{1-b})^n \quad (44)$$

The rate of increase of α_n proceeds as $n(\frac{1+b}{1-b})^n$ when $n < p+1$ which is somewhat faster than the rate when $n > p+1$. This seems to agree with the original experiments of Wilhelm et al.⁽³⁾ (see Figure 4). The above equilibrium analysis is applicable only when the full reservoirs (no dead volume) are displaced in such a way that $L_c < L_H \leq h$, which prevents solute mixing between reservoirs (Region I according to Chen and Hill⁽⁹⁾). Chen and Hill have treated the case when the existence of dead volume is important. The solution of this problem will be rederived in a later section. The effect of using purely sinusoidal potentials has also been considered⁽¹³⁾ and suggests that the rate of enrichment is less than for square potentials. This study points out that sinusoidal bed temperature cycle can be thought to represent a thermal dissipation effect, since square temperature waves applied to the bed jacket will appear more nearly sinusoidal in the bed center owing to thermal dissipation effects. This provides a convenient method of introducing dissipation into the equilibrium model, especially useful for gaseous separations.

Inspection of equations (43) and (44) shows that separation factor for $n < p+1$ is independent of p and q and depends only on b . Later, when $n \geq p+1$, the separation factor depends on p , q and b . For the latter case, a single data point cannot be used to estimate b in the manner of Pigford et al.⁽⁸⁾. However, for $n < p+1$ and $b \ll 1$, a useful asymptotic relationship results

$$\ln \alpha_n \approx \text{constant} + n \ln \left(\frac{1+b}{1-b} \right) \quad (45)$$

This shows that $\ln \alpha_n$ is approximately linear in n with slope $\ln \left(\frac{1+b}{1-b} \right)$. Figure 4 shows that the original data of Wilhelm et al.⁽³⁾ seems to obey this simple form in the early period of cycling. Values of p and q can be estimated from experiments for $n \gg p+1$ by noting

$$\ln \alpha_n \approx \ln \left[1 + q + \frac{2b}{1+b} p + \left(\frac{1-b}{1+b} \right) (1-q) \right] + n \ln \left(\frac{1+b}{1-b} \right)$$

These asymptotic results may be useful for parameter estimation in well-behaved systems. The researcher is cautioned to

note that after a large number of cycles one expects to produce a large axial gradient giving rise to a strong dissipative effect associated with axial mixing. One expects the above asymptotic result will lead to a value of b which is smaller than the value obtained from a small number of cycles. By including such dissipative effects in the parameter b , one can easily imagine a model which incorporates a time-varying Murphree-type tray efficiency. This would seem to be a very promising avenue to explore for batch systems, especially if practical, easy-to-apply system equations are the aim. However, it would seem the linear non-equilibrium rate equations (7) and (8), coupled with a linear equilibrium relation (eq. 9) are not intractable, and pose one of the unsolved analysis problems in contemporary chemical engineering. As a start, one would expect to obtain first approximations to the analytical solution using a singular perturbation technique.

Effect of Reservoir Dead Volume on the Equilibrium Theory of DTM

In the original equilibrium theory of direct-thermal-mode (DTM), Pigford et al.⁽⁸⁾ and later Aris⁽¹⁰⁾ assumed no dead volume exists in the perfectly mixed top and bottom reservoirs. Pumping commenced with one reservoir completely full (and fully displaced during a half-cycle) while the other is initially empty. In real systems, some dead volume (undisplaced reservoir volume) is always present, for example in connecting lines and flow distributors.

The equilibrium theory was extended to include dead volume by Chen and Hill⁽⁹⁾ (using the nomenclature of Pigford et al.) and also an attempt was made to consider this problem by Gregory and Sweed⁽¹⁴⁾ at an earlier date. We continue to build on the Pigford et al. solution derived earlier (using their nomenclature) and re-derive the solution of Chen and Hill, the details of which were not given in their original paper⁽⁹⁾. As pointed out by Wankat⁽⁷⁾, the Gregory-Sweed solution for dead volume effects do not appear to agree with the results of Chen and Hill⁽⁹⁾. We note here that the presence of dead volume does not affect the ultimate reservoir compositions, but only the transient approach to steady-state.

Obviously, the larger the reservoirs relative to the column interstitial fluid, the longer it takes to reach steady-state.

We build on the previous system equations (c.f. eq. 35) and solutions (e.g. eq. 41) and note that we must also write a system of external equations to reflect the fact that reservoir contents are not completely displaced. Furthermore we must take note of the fact that a particular reservoir composition at beginning and end of a cycle are distinctly different, hence an additional notation must be introduced.

Building on the nomenclature in Figure 5, the following definitions are necessary:

$\langle y_{TH} \rangle_n$ = contribution to top reservoir composition injected during hot n^{th} half-cycle.

$\langle y_{TC} \rangle_n$ = mixed top reservoir composition injected down during the cold n^{th} half cycle.

$\langle y_{BH} \rangle_n$ = mixed bottom reservoir composition injected during the hot n^{th} half-cycle.

$\langle y_{BC} \rangle_n$ = contribution to bottom reservoir composition injected during the cold n^{th} half-cycle.

Penetration distances are defined the same as before (L_C , L_H , see eqs. (23) and (24)) and the parameters p and q are defined as in eq. (33) and the discussion following thereafter.

The internal equations are now modified to read (compare with eq. (30) and (35)) for the top reservoir

$$\begin{aligned} \langle y_{TH} \rangle_n &= \frac{AB}{AD} \left(\frac{1+b}{1-b} \right) \langle y_{TC} \rangle_{n-1} \\ &+ \frac{BC}{AD} \langle y_{BH} \rangle_{n-p-1} + \frac{CD}{AD} \langle y_{BH} \rangle_{n-p} \end{aligned} \quad (46)$$

Note that $\langle y_{TC} \rangle_n$ is the composition, while $\langle y_{TH} \rangle_n$ is a contribution. In the bottom reservoir we have:

$$\langle y_{BC} \rangle_n = \frac{1-b}{1+b} \langle y_{BH} \rangle_n \quad (47)$$

where again $\langle y_{BH} \rangle_n$ is the reservoir composition, while $\langle y_{BC} \rangle_n$ is a contribution.

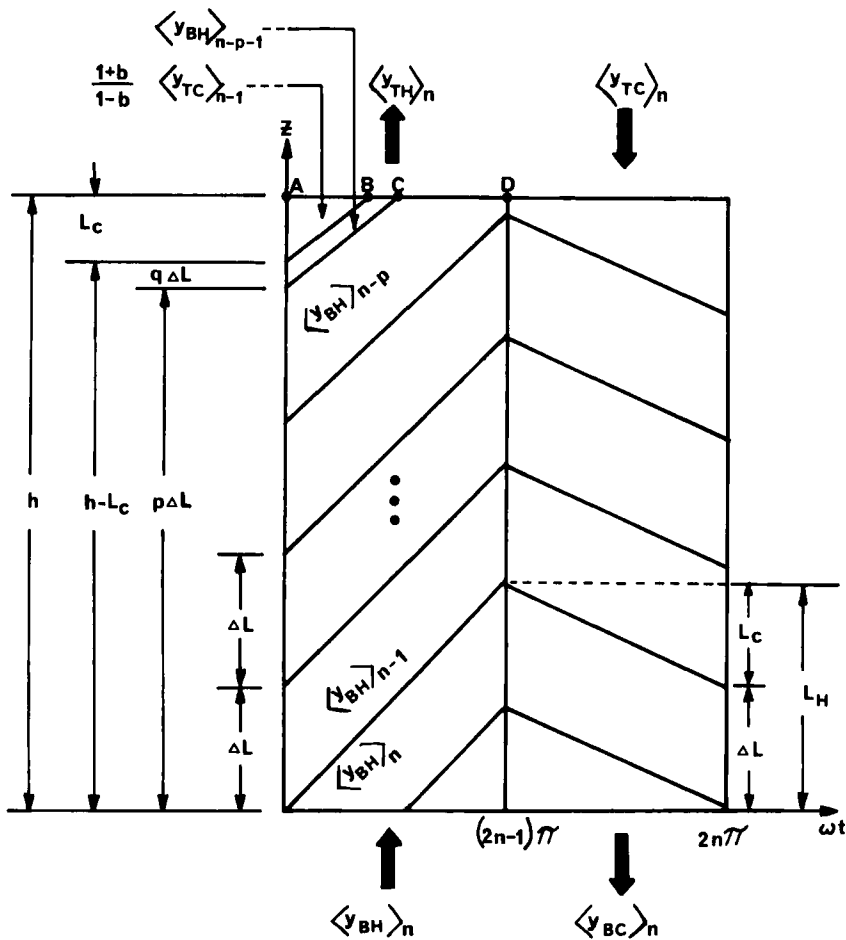


FIGURE 5

Characteristics for batch or continuous pumps containing dead-volume

The external equations comprise a solute balance on the reservoirs, and for the top we have

$$Q \frac{\pi}{\omega} \langle y_{TH} \rangle_n + V_T \langle y_{TC} \rangle_{n-1} = (V_T + Q \frac{\pi}{\omega}) \langle y_{TC} \rangle_n \quad (48)$$

The first term on the LHS is the amount injected into upper reservoir at the end of n^{th} hot half-cycle; the second term is the amount left over from previous $(n-1)^{\text{th}}$ cold cycle; the sum of these equals the solute contents of the top reservoir beginning the n^{th} cold (downflow) cycle. Similarly for the bottom reservoir

$$\langle y_{BC} \rangle_{n-1} \frac{Q \pi}{\omega} + V_B \langle y_{BH} \rangle_{n-1} = (V_B + Q \frac{\pi}{\omega}) \langle y_{BH} \rangle_n \quad (49)$$

Thus, we have a finite difference system of four equations and four unknowns. The initial condition is y_0 as before. The above system of equations are identical to Chen and Hill, except for the subscripts H and C, where Chen and Hill used 1 and 2 respectively. However, Chen and Hill did not explain their nomenclature, especially the distinction between *composition* and *contribution*. This has perhaps contributed to the skepticism of the work in a recent review by Wankat⁽⁷⁾.

As before, we make the distinction between cases where $n > p$ and $n < p$. For $n < p$, equation (46) is rewritten noting that all subscripts \leq zero on the RHS are replaced with y_0 , hence

$$\langle y_{TH} \rangle_n = \langle y_{TC} \rangle_{n-1} + \frac{2b}{1+b} y_0 \quad (50)$$

where the fractions AB/AD, BC/AD, etc. are the same as given earlier in eq. (33).

The compositions we seek are $\langle y_{TC} \rangle_n$ and $\langle y_{BH} \rangle_n$. This compares with $\langle y_{T2} \rangle_n$ and $\langle y_{B1} \rangle_n$ in the Chen-Hill nomenclature. These workers give $\langle y_{B2} \rangle_n$, which is not a reservoir composition, but a contribution, hence of no value.

We first solve eq. (50) coupled with the external equation (48) to eliminate $\langle y_{TH} \rangle_n$ giving

$$\langle y_{TC} \rangle_n - \langle y_{TC} \rangle_{n-1} = y_0 \frac{2b}{1+b} \frac{Q \pi / \omega}{V_T + Q \pi / \omega} \quad (51)$$

which is easily solved to give

$$\langle y_{TC} \rangle_n = B + y_0 \left(\frac{2b}{1+b} \right) \frac{Q \pi / \omega}{V_T + Q \pi / \omega} n$$

Applying the initial condition to find B gives for $n < p$:

$$\frac{\langle y_{TC} \rangle_n}{y_0} = 1 + (n-1) \left[\frac{2b}{1+b} \frac{Q \pi/\omega}{V_T + Q \pi/\omega} \right] \quad (52)$$

which is identical to the result of Chen and Hill.

We next solve for $\langle y_{BH} \rangle_n$ by combining eqs. (47) and (49) to give

$$\langle y_{BH} \rangle_n - \left[\frac{\frac{(1-b)}{(1+b)} Q \pi/\omega + V_B}{V_B + Q \pi/\omega} \right] \langle y_{BH} \rangle_{n-1} = 0 \quad (53)$$

The initial condition on $\langle y_{BH} \rangle_n$ is y_0 at $n=1$, hence for $n \geq 1$:

$$\frac{\langle y_{BH} \rangle_n}{y_0} = \left[\frac{\frac{(1-b)}{(1+b)} Q \pi/\omega + V_B}{V_B + Q \pi/\omega} \right]^{n-1} = \beta^{n-1} \quad (54)$$

where we introduce the eigenvalue β for the dead volume case. We next insert the above expression into eq. (46) and use eq. (48) to eliminate $\langle y_{TH} \rangle_n$ to give for $n > p$:

$$\begin{aligned} \langle y_{TC} \rangle_n - \langle y_{TC} \rangle_{n-1} &= y_0 \left(\frac{Q \pi/\omega}{V_T + Q \pi/\omega} \right) \frac{2b}{1+b} [q\beta^{n-p-2} \right. \\ &\quad \left. + (1-q)\beta^{n-p-1}] \end{aligned} \quad (55)$$

This has a solution of the form

$$\langle y_{TC} \rangle_n = A + y_0 \frac{Q \pi/\omega}{V_T + Q \pi/\omega} \frac{2b}{1+b} \left[\frac{q\beta^{n-p-1}}{\beta-1} + \frac{(1-q)\beta^{n-p}}{\beta-1} \right] \quad (56)$$

We require that the two solutions, eq. (52) and eq. (56), are equal at $n=p+1$, if q is finite, providing a condition to find the constant A . Evaluating A in this way, we obtain

$$A = y_0 \left[1 + \frac{2b}{1+b} \frac{Q \pi/\omega}{V_T + Q \pi/\omega} \left(p - \frac{q + (1-q)\beta}{\beta-1} \right) \right] \quad (57)$$

The top composition with dead volume can now be determined for $n \geq p+1$, giving

$$\frac{\langle y_{TC} \rangle_n}{y_0} = 1 + \frac{2b}{1+b} \frac{Q \pi/\omega}{V_T + Q \pi/\omega} \left\{ p + \frac{1}{1-\beta} (q + \beta(1-q)) (1 - \beta^{n-p-1}) \right\} \quad (58)$$

This relationship is identical to that presented without derivation by Chen and Hill⁽⁹⁾. The bottom composition is given by eq.

(54), hence the separation factor for $n \geq p+1$ is obtained by dividing eq. (58) by eq. (54).

One would expect in the limit as $V_T, V_B \rightarrow 0$ that the relationship for $\langle y_{TC} \rangle_n$ should become identical to the no-dead-volume situation, described by eq. (41). This is not the case because without dead-volume, the feed to the column during upstroke is $\langle y_B \rangle_{n-1}$. This is not accounted for in the mathematics leading to eq. (58). However, if the bracketed expression $(1-\beta^{n-p-1})$ in eq. (58) is incremented downward to read $(\beta^{-1} - \beta^{n-p-2})$ then the results become identical. There has been considerable confusion regarding the differing results obtained by separate research groups. The confusion arises mainly as consequence of incompletely explained nomenclature. Except for the minor corrections noted, the results now appear to be consistent and correct.

Rate Considerations in DTM

The equilibrium theory⁽⁸⁾ cannot predict the ultimate separation ($t \rightarrow \infty$) in parapumps, but seems to be a good predictor of events occurring in the early stages of separation. Dissipative effects (which are ignored in the equilibrium theory) tend to limit the maximum separation obtainable. This important aspect will be treated in a separate section entitled Ultimate Separation.

We now pose one of the unsolved analytical problems in para-pumping. The simplest dissipative effect we can incorporate in the equilibrium model is a mass transfer resistance between flowing fluid and solid adsorbent. Under each conditions, the non-dispersive solute balance on the fluid plus solid becomes (c.f. eqs. (7) and (8)):

$$\epsilon_b \rho_f \frac{\partial y}{\partial t} + \bar{\rho}_s (1-\epsilon_b) \frac{\partial x}{\partial t} + \rho_f V \frac{\partial y}{\partial z} = 0 \quad (59)$$

and the solute balance on the solid phase alone gives the rate expression

$$\rho_s (1-\epsilon_b) \frac{\partial x}{\partial t} = k_m a_p (y - y^*) \rho_f \quad (60)$$

The mass transfer coefficient, k_m , can also include effects associated with pore diffusion⁽¹⁵⁾. Finally, one must pose an equilibrium relationship

$$x = f(y^*, T) \quad (61)$$

This system of equations is linear if a linear isotherm is applicable, i.e.,

$$z = M(t) y^* \quad (62)$$

Rhee and Amundson⁽¹⁶⁾ suggest deviations from the equilibrium theory are due more to the non-linearity of the isotherm (pinch regions) than to mass transfer resistance. This poses an interesting problem, since all isotherms intersect in at least one point where x and y^* are identically zero. However, because of the low velocities prevailing in parapumps, one also expects the mass transfer resistance to be large. What we conclude from these considerations is as follows. In the early cycling period, the equilibrium theory seems to adequately predict the rate of separation, especially for open, continuous systems (to be discussed shortly). In the medium time regime, local effects arising from transfer resistance would seem to limit separation. In the long time regime, one would speculate that global effects associated with the non-linearity of isotherms and large axial gradients may control the separation. The last statement leads to the consideration of a possible graphical procedure⁽¹⁶⁾ for calculating stages (cycle number) for a given separation. Such a procedure was indeed used by Wakao, et al.⁽¹⁷⁾ in a paper which predates the comprehensive work of Wilhelm et al.⁽³⁾. Attempts have been made (notably by Hung and Lee⁽¹⁸⁾) to use a staging concept, but a general graphical technique coupled with a tray-efficiency concept (to reflect local deviations from equilibrium) has yet to be published. Such design techniques have received scant attention in the literature and bear reexamination. The important practical issues raised by Harris⁽¹⁹⁾ should also be given careful consideration.

A numerical solution of eqs 59-61 for the DTM was presented by Wilhelm et al.⁽³⁾ Sometime later, Sweed and Wilhelm⁽¹²⁾ published a more efficient numerical calculation procedure, called the STOP-GO algorithm. In this paper, the numerical solution of eqs. (59) to (61) was compared with experiments conducted using the system toluene, n-heptane on silica gel. After suitable parameter estimation (the dead volume and transport coefficient were manipulated), a good fit of theory and experiment evolved. It is important to note that as much as five times the actual experimental dead volume was necessary in the model simulation to obtain a good fit. Since the presence of dead volume is not supposed to influence the ultimate separation, it would have been instructive had the authors used actual dead volume and then tried to predict the ultimate separation by suitably manipulating transfer coefficients. In short, did the ultimate separation predicted by the model equations depend on the size chosen for the dead volume? If so, the model would be suspect. In any case, care must be exercised in using such models for 'a priori' design purposes.

The Recuperative Mode of Parapumping

The original description of parapumping by Wilhelm, Rice and Bendelius⁽¹⁾ proposed a method of cyclic adsorption-desorption which has since been named the Recuperative Mode⁽³⁾. Instead of adding or extracting heat through the walls of the column, the slug of fluid entering the column is either heated (upflow) or cooled (downflow). Otherwise, the mathematical description of the process and the mechanism for separation is the same as the direct mode. According to Gregory⁽²⁰⁾ the advantage of the recuperative mode is that it avoids the difficult heat transfer problem of the direct mode for large-scale equipment. This may be a fictitious advantage, since one could use many small tubes (such as multi-tube shell heat exchanger) in a large scale direct mode device. The recuperative mode does seem to make the heat recovery problem easier, but since degraded forms of energy are usually used in the first instance,

the advantage is of marginal consequence. Finally, while the actual separations obtained so far using the recuperative mode have not been impressive ($\alpha = 1.17$ for the NaCl system studied by Rolke and Wilhelm⁽²¹⁾), there is an inherent disadvantage to this mode of operation which has not been fully discussed in the literature. To use the maximum available adsorbent surface area in a recuperative system, one must displace the entire interstitial volume of the column. This insures that all the packing particles undergo a temperature cycle. However, it has been shown experimentally^(3,12) and recently explained theoretically^(15,22) that large fluid displacements induce strong dissipative effects which limit separation. The direct mode, on the other hand, can be effectively operated with small fluid displacements, thus building a much larger axial concentration gradient, at the expense necessarily of production rate.

While the future for the recuperative mode does not appear promising, a scheme whereby shallow bed recuperative devices are staged in a series fashion with inter-coolers/heaters linked in a countercurrent arrangement (for maximum heat recovery) may be a viable proposition. On leaving the subject, we should point out that the modeling techniques and parameter estimation experiments of Rolke and Wilhelm⁽²¹⁾ are perhaps the most complete and mathematically rigorous treatment on the subject of parapumping to date. It is unfortunate that the system chosen produced such modest separations, since this appeared to discourage further experimentation on the technique.

Design Considerations and Ultimate Separation in Batch Parapumps

Except for the comments put forth by Harris⁽¹⁹⁾, the question of equipment size has received scant attention in the literature. Recently^(15,22,23,24), there have been attempts using first principles to come to grips with this important question for batch systems. In these works, the analysis focuses attention on the ultimate separation. This is the state in a batch system where

the time-average reservoir compositions are stationary, hence the time-average flux along the column axis is nil. All real batch systems reach an ultimate separation, since all systems have dispersive forces acting. The types of dispersive forces introduced into a model of the ultimate separation determines the various length and time scales necessary to reach (as time $\rightarrow \infty$) a given separation. Furthermore, one expects that for zero frequency of operation no separation results; at the other extreme (infinite frequency) no separation is expected. At the outset, then, one suspects there may exist a maxima or minima (or both) in separation factor as frequency is increased.

This approach was used very recently by Foo and Rice⁽¹⁵⁾ to evolve simple design relations for batch parapumps, and also to see if there exists an optimum frequency for maximum ultimate separation.

The fundamental relationship uncovered for purely sinusoidal velocity and temperature fields was found to be of simple structure, namely

$$\ln \alpha_{\infty} = \frac{(L/R)^2 (Pe_m) (A/L) \operatorname{Real}(\psi_1)}{E/D + \frac{1}{2} (A/L Pe_m L/R)^2 \operatorname{Real}(\psi_2)} \quad (63)$$

Here, α_{∞} is the ultimate separation factor as $t \rightarrow \infty$. The important dimensionless groups in this relationship are length of packing/radius of column (L/R), fluid displacement/length of packing (A/L), and dimensionless frequency (Peclet number, $Pe_m = R^2 \omega / D$). The complex transcendental functions take two distinct forms according to whether effects owing to pore diffusion are lumped into the film transfer coefficient, or described exactly by solving the dynamic diffusion equation in spherical coordinates. The several transcendental relationships for ψ_1 and ψ_2 are given elsewhere⁽¹⁵⁾, but a simplified version will be given shortly. When pore diffusion is unimportant, and film resistance along with axial mixing are the key dissipative effects, the following simplified relationship results when thermal response is fast:

$$\text{Real } \psi_1 = \frac{1}{2} \left(\Delta T \frac{\alpha_b |k_1|}{\delta} \right) \text{Sh}^2 / \left[\left(\frac{1-\delta}{\delta} \right)^2 \text{Pe}_m^2 + \text{Sh}^2 \right] \quad (64)$$

$$\text{Real } \psi_2 = \text{Sh}(\delta-1)^2 / (\text{Sh}^2 \delta^2 + (\delta-1)^2 \text{Pe}_m^2) \quad (65)$$

where the dimensionless capacitance factor δ is

$$\delta = \alpha_b (k_0 + k_1 \bar{T}) + 1 + \epsilon_p (1 - \epsilon_b) / \epsilon_b \quad (66)$$

and \bar{T} is the average bed temperature.

The solids hold-up α_b is given by:

$$\alpha_b = \rho_s (1 - \epsilon_b) (1 - \epsilon_p) / \epsilon_b \quad (67)$$

The linear adsorption rate factors (k_0, k_1) arise from assuming an isotherm that obeys

$$q = k^* c^* = (k_0 + k_1 T) c^* \quad (68)$$

where for normal isotherms k_1 is expected to be negative. The Sherwood number in this work is taken to be

$$\text{Sh} = k_m a_p R^2 / \epsilon_b D \quad (69)$$

and depends on the specific form selected for the film coefficient (among a selection of many, see Foo and Rice⁽¹⁵⁾).

Asymptotic results useful for predicting behavior when $\text{Pe}_m > \text{Pe}_{m,\text{opt}}$ can be deduced by considering the case when $\text{Sh} \gg \text{Pe}_m$, that is when $k_m a_p \gg \omega$. For these conditions, we obtain

$$\text{Real } \psi_1 \approx \frac{1}{2} \frac{\Delta T \alpha_b |k_1|}{\delta} \quad (70)$$

and

$$\text{Real } \psi_1 \approx \left(\frac{\delta-1}{\delta} \right)^2 / \text{Sh} \quad (71)$$

When these are inserted in the fundamental separation factor relationship, eq. (63), an asymptotic expression to estimate separation factors can be shown to be:

$$\ln \alpha_\infty \approx \frac{\left(L/R \right)^2 \left(\text{Pe}_m \right) \left(A/L \right) \left(\frac{1}{2} \frac{\Delta T \alpha_b |k_1|}{\delta} \right)}{E/D + \frac{1}{2} \left(A/L \right) \left(\text{Pe}_m \right) \left(L/R \right)^2 \left(\frac{\delta-1}{\delta} \right)^2 / \text{Sh}} \quad (72)$$

For large columns, the ratio of dispersion coefficient to molecular diffusion (E/D) is expected to be significant. The design curves given in Figure 6 were determined using mass transfer coefficients after Wakao et al. (25):

$$k_m D_s / D = 2 + 1.45 \text{ Re}^{1/2} S_c^{1/3} \quad (73)$$

where the RMS velocity was used in computing Reynolds number.

Dispersion was determined after the work of Klinkenberg and Sjenitzu (26):

$$E/D = 1 + \frac{3}{\sqrt{2}} (D_s/R)(L/R)(A/L)Pe_m \quad (74)$$

A simple linear equation for parameter estimation purposes can be obtained by inverting eq. (72) and letting the second term in eq. (74) dominate axial dispersion, giving

$$1/\ln \alpha_\infty \approx a_0 (Pe_m A/L/Sh) + b_0 \quad (75)$$

where

$$a_0 = \left(\frac{\delta-1}{\delta}\right)^2 \delta/\Delta T \alpha_b |k_1|$$

$$b_0 = \frac{6}{\sqrt{2}} (D_s/R)/[(L/R) \Delta T \alpha_b |k_1|/\delta]$$

It was shown by Foo and Rice (15) that a variety of experimental and simulated data seemed to obey the simple approximate solution represented by eq. (75). For an equilibrium situation ($Sh \rightarrow \infty$) with no axial dispersion ($E/D \rightarrow 0$), eqs. (72) or (75) show that $\alpha_\infty \rightarrow \infty$, as Pigford et al. (8) have previously shown.

Inspection of the curves in Figure 6 shows that a maximum separation factor occurs as frequency is increased. The Peclet number corresponding to the maximum depends strongly on the selection of fluid displacement (A/L) and weakly on the Schmidt number. At high frequency ($Pe_m > 10^2$), a reversed (and highly attenuated) separation occurs. This aspect is discussed more fully elsewhere (15,27); suffice to say separation factors predicted for this region are quite small and operation there is not recommended.

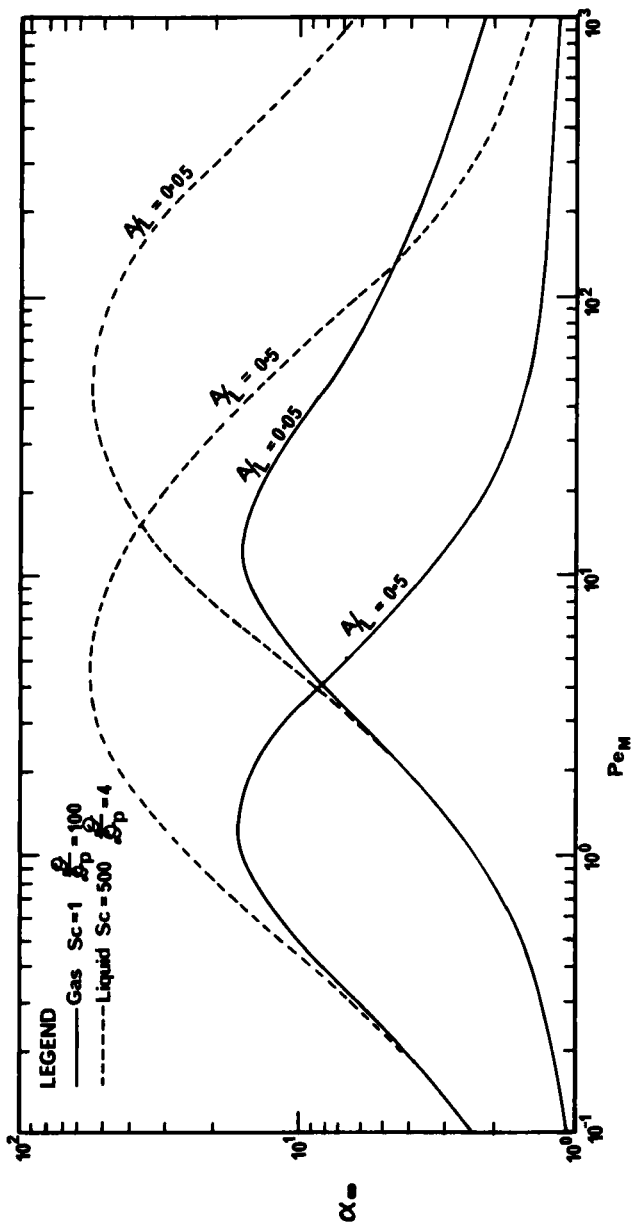


FIGURE 6

Ultimate separation factors; curves were computed using $k_o = 2.56 \frac{cc}{\text{gram}^o_F}$, $k_1 = -0.02 \frac{cc}{\text{gram}^o_F}$, $\varepsilon_b = 0.5$, $\varepsilon_p = 0.5$, $T_h - T_c = 100^oF$, $L/R = 100$, $R/R_s = 10$, $\bar{T} = 82^oF$, $\rho_s = 2 \text{ gram/cc}$

A simple asymptotic design equation evolves when the only dispersive forces are axial mixing and film mass transfer resistance. Thus, rearranging the asymptotic result given by Eq. (72) gives simply

$$\ln \alpha_{\infty} \approx \frac{(AL\omega) \left(\frac{1}{2} \Delta T \alpha_b |k_1| / \delta \right)}{E + \frac{1}{2} \left(\frac{A^2 \omega^2 \epsilon_b}{k_m a_p} \right) \left(\frac{\delta-1}{\delta} \right)^2} \quad (76)$$

which is independent of column diameter, provided diameter does not enter via E or $k_m a_p$. The above relationship does not hold when pore diffusion is important, since for such cases there is a temptation to use (Foo and Rice⁽¹⁵⁾) a lumped transport coefficient which reflects pore diffusion, i.e.

$$k_m a_p \Big|_{\text{pore}} = \frac{60 D_p \epsilon_p (1 - \epsilon_b)}{D_s^2} \quad (77)$$

which usually gives $k_m a_p$ of order ω . The development of asymptotic results in eqs. (72) and (76) depend on the condition that $Sh \gg Pe_m$, that is $k_m a_p \gg \omega$. However, if the complete forms for ψ_1 and ψ_2 are used from eqs. (64) and (65), then pore diffusion can be embedded in the Sherwood number using eq. (77). The reader is cautioned to remember that thermal response has not been included in this simplified analysis, and may be important, especially for gaseous separations on dense adsorbent.

Consider the following preliminary design calculation. Suppose we take the Sweed-Gregory⁽²⁸⁾ system where ion retardation resin (Bio-Rad Ag11A8) was used to study the desalination of water. The hot and cold temperatures used were 131°F and 41°F, respectively, giving a thermal driving force $\Delta T = 90^\circ\text{F}$ at a mean temperature of 86°F. The linear equilibrium coefficient (eq. 68) varied with temperature to give approximate values of 2 cc/gram and 1.5 cc/gram at 41°F and 131°F, respectively. The calculated constants for eq. (76) are $k_0 = 2.23$ cc/gram and $k_1 = -5.6 \times 10^{-3}$ cc/gram-°F. Voidages for column and pores are each taken to be one-half, and the packing diameter is around 0.1 cm. The compressed

solids density (ρ_s) is estimated to be 0.8 g/cc. The above information allows the parameters α_b and δ to be computed as 0.4 g/cc and 2.2, respectively. It was stated by these workers that pore diffusion and film resistance were both important in the system studied. In the following design calculation, we include only film resistance using eq. (73), which is approximated by

$$k_m \approx 1.45 \left(\frac{A\omega}{D_s \sqrt{2}} \right)^{1/2} D^{2/3} / \nu^{1/6} \quad (78)$$

At the outset, the design is expected to be undersized. Since it has been suggested⁽²⁹⁾ the only effective external mass transfer area is pore area, the packing factor is calculated from:

$$a_p = \frac{6\epsilon_p (1-\epsilon_b)}{D_s} \quad (79)$$

Axial mixing is estimated from eq. (74) giving approximately

$$E \approx \frac{3}{\sqrt{2}} A D_s \omega \quad (80)$$

We consider a specific experimental result of Sweed-Gregory⁽²⁸⁾ whereby $A/L = 0.8$ and the cycle time used was 20 minutes ($\omega = 5.23 \times 10^{-3}$ rad/sec). Under these conditions, an ultimate separation factor of 3.4 was obtained. Inserting the above information into eq. (76), with "L" taken as the unknown, the following algebraic equation results:

$$L - 3.9652 L^{1/2} - 5.647 = 0 \quad (81)$$

which is quadratic in $L^{1/2}$. The calculated column height is found to be:

$$L = 26 \text{ cm} \quad (82)$$

which should be compared with the 60 cm of packed height actually installed by Sweed and Gregory⁽²⁸⁾. The column design is undersized since the important dissipative effect owing to pore diffusion has been neglected. However, for preliminary screening purposes the above simplification should be considered entirely adequate. The final design can be accomplished using eq. (63), including the dynamics associated with pore diffusion given elsewhere

(15). A simpler approach is to use the complete functions expressed in eqs. (64) and (65), and mass transfer coefficient which includes pore diffusion such as eq. (77).

The key parameter in the design calculation is the equilibrium temperature coefficient $|k_1|$, since $\frac{|k_1|\Delta T}{\delta}$ is the driving force for separation. What we see here is an underlying, but simple, driving force for separation which depends essentially on the average difference in the adsorption equilibrium curves at the two temperatures. The group of parameters $\Delta T|k_1|/\delta$ has essentially the same significance as the parameter "b" introduced by Pigford et al. (8). To see this, we note that k^* in eq. (68) is equivalent to M/ρ_f in eq. (9), hence the following result is obtained

$$m = k^* \rho_s (1 - \epsilon_b) / \epsilon_b$$

and from eq. (17)

$$a = \frac{k_1 \Delta T \rho_s (1 - \epsilon_b)}{\epsilon_b}$$

which gives the equivalence

$$b = \frac{k_1 \Delta T \rho_s (1 - \epsilon_b) / \epsilon_b}{1 + \frac{\rho_s (1 - \epsilon_b)}{\epsilon_b} (k_0 + k_1 T)} \quad (83)$$

The above analysis was originally⁽¹⁵⁾ derived by using purely sinusoidal driving potentials, i.e.

$$v = v_{os} \sin \omega t$$

where normally square potentials are used⁽⁸⁾

$$v = v_0 \operatorname{sq}(\omega t)$$

To use the previous design relations for conditions of square velocity potential, the displacements should be made equivalent, that is

$$v_{os} \int_0^{\pi/\omega} \sin \omega t \, dt = v_0 \left(\frac{\pi}{\omega} \right) \quad (84)$$

which requires

$$v_{os} = \frac{\pi}{2} v_0$$

and since $v_0 = A/(\pi/\omega)$ (that is displacement length divided by half-cycle time), the equivalent velocity is

$$v_{os} = A \omega/2 \quad (85)$$

where A denotes displacement for a square velocity wave.

Recent Applications and Ideas

Hamrin and co-workers^(30,31,32) at the University of Kentucky have applied the DTM to several novel systems. In addition to the DTM work, hydrogen isotopes were continuously separated in the gas phase using heatless adsorption⁽³³⁾ using a processing scheme similar to parametric pumping.

The separation of gaseous Boron isotopes was reported by Schroeder and Hansin⁽³¹⁾, however the separation factors obtained (1.02 to 1.028) were quite small. In another novel application, Shaffer and Hamrin⁽³⁰⁾ obtained enzyme separations using cyclic pH to promote the retardation-release mechanism. A batch DTM to separate SO₂ from air was reported by Patrick, Schrottd and Kermode⁽³²⁾ to give separation factors up to 130.

Chen, Lin, Stoker and Fabisiak⁽³⁴⁾ used continuous DTM to separate a multicomponent mixture of toluene, aniline-n-heptane on silica gel. This effort will be discussed more fully in the section on open systems.

Thompson and co-workers^(4,5) at the University of British Columbia used electrosorption-desorption to separate NaCl from water in batch and continuous systems. Separation factors for the best batch system⁽²⁵⁾ were reported to be large ($>10^3$). Operation is exactly analogous to the DTM parapump, except retardation is accomplished by ion-selective membranes, ion injection to the membranes being induced by an applied electric potential. The release (desorption) mechanism is accomplished by reversing potential. The basic strategy of the process is the same as parapumping, and in fact Wilhelm and co-workers⁽³⁾ envisaged an intensive variable such as electricity or magnetism to cause the essential retard-

release mechanism. Several new ideas were implemented in the original paper by Thompson and Bass⁽⁴⁾. One of their important experimental innovations was to divide a half-cycle into unequal pause-flow increments. This idea would seem to be worth applying to thermal parapumps, since mass transfer coefficient depends strongly on temperature (roughly as $T^{3/2}$ for liquids), hence film resistance differs significantly for hot and cold cycle.

In connection with an electrosorption retardation mechanism, Lee and Kirwan⁽⁶⁾ have very recently shown that certain biological molecules (e.g., glucoamylase) are selectively adsorbed on carbon and the amount adsorbed depends upon the direction of applied voltage.

The problem of parametric pumping as a candidate model for active human cell transport has recently been reconsidered. Posed originally by Wilhelm⁽³⁵⁾, the parapump model of active cell transport was criticized by Booij⁽³⁶⁾ because of a length and time scale problem; that is scaling down from laboratory apparatus of length 50-100 cm, to biomembrane thicknesses of 50-100 Å and from parapump frequencies of 10^{-3} Hz to a living cell frequency expected in the range of 10^6 - 10^8 Hz. In a recent exchange of correspondence⁽³⁷⁾, Rice provided an order of magnitude analysis for this scaling problem based on the theoretical result⁽²⁴⁾ that maximum parapump separations lie in a range where the Peclet number is:

$$1 \leq \left(\frac{A r_0 \omega}{D} \right) \leq 3$$

An order of magnitude calculation using $\omega = 2\pi 10^7$ Hz, $A \approx r_0$ (fluid displacement equals pore radius) and molecular diffusion $\approx 10^{-5}$ cm²/sec, gave a conservative estimate of pore radius as 69°. This result was criticized by Booij⁽³⁶⁾ who contended '... the pore size should be 7 Å at the utmost.' Because of the range of lengths and frequencies originally suggested by Booij⁽³⁶⁾, one can easily select the most favorable of the suggested conditions to see if a pore size < 7 Å can be calculated. Taking $A \approx 100$ Å, $\omega = 2\pi 10^8$ Hz, $D \approx 10^{-5}$ cm²/sec and $\frac{A r_0 \omega}{D} \approx 1$, there results

$$r_0 = \frac{10^{-5}}{6.28 \times 10^8 \cdot 100/10^8} = 1.6 \times 10^{-8} \text{ cm} = 1.6 \text{ \AA}$$

Thus, the precise outcome of the calculation depends on the particular selection of the physical variables suggested by Booij in the first instance. The real point of the exercise is an order of magnitude analysis, and this was not appreciated by Booij⁽³⁸⁾. If the original physical estimates stated by Booij⁽³⁶⁾ are correct, the candidacy for the parapump model of active cell transport cannot be dismissed on the grounds of frequency and length scale.

A novel application of parapumping has recently appeared⁽³⁹⁾ where it is proposed to let the device serve as a catalytic chemical reactor. This approach applied to a single pore with reversible reaction occurring at the pore wall may be worth applying to the active human cell transport problem, where the equilibrium constant associated with the reversible reaction may be controlled, perhaps, by electrical potential. In the paper by Apostolopoulos⁽³⁹⁾, a near-equilibrium approach was used to model the chemical parapump. This work leads to the conjecture that a single unit could serve as reactor and separator. The work also undertakes to use a Murphree-type stage efficiency (deviation from equilibrium) to explain the excursions of experimental separations from the Equilibrium Theory. There are several ideas which deserve careful consideration in this paper.

Horn and Lin⁽⁴⁰⁾ have discussed the analogy between the "induced transport" associated with parapumping and conventional separation methods. The enrichment problem is shown to have the dual-temperature process as the steady counter-part, and the splitting (stripping) problem is shown to be analogous to extraction. In this regard, Wankat⁽⁴¹⁾ has reported experiments on a liquid-liquid extraction parametric pump, but separation factors are quite small. However, theoretical predictions indicate promising possibilities if the practical problems can be overcome.

Open Systems

Open systems are operated in such a way that feed is injected and product (or products) are removed in a continuous or semi-continuous way. Several arrangements for accomplishing this purpose are shown in Figure 7. The oscillating U-tube arrangement in this figure (or back-to-back parapump after Thompson and Bowen⁽¹¹⁾) would appear to offer several advantages⁽⁴²⁾. First, the leak problem associated with reciprocating pistons is eliminated, as well as the initial costs associated with purchasing a pulsed flow device (e.g. infusion-withdrawal pumps). Secondly, the device can easily be used in a batch or continuous mode of operation. Finally, the device is easily staged using gravity as the means of obtaining periodic flow.

Two theoretical treatments of the equilibrium open system have appeared, namely that of Chen and Hill⁽⁹⁾ and Gregory and Sweed^(14, 43). Chen and co-workers^(44,45) have also tested their theory on experimental systems, including a multi-component separation⁽³⁴⁾. Because Chen and Hill⁽⁹⁾ used the nomenclature of Pigford et al.⁽⁸⁾ and for the sake of consistency, we continue to use their theoretical development for open systems. There is some controversy regarding the consistency of the Chen-Hill theoretical results, hence we rederive the model predictions for the most important case with feed at the top and $L_c < L_h < h$ which assures complete solute removal. Actually, complete separation is assured as long as the cold solute front does not penetrate into the lower reservoir, that is $L_c < h$ (Region I⁽⁹⁾). The development follows along the lines leading up to eq. (58), with particular reference to Figure 5. The internal transport relations are the same as represented by eq. (46) for the upflow and eq. (47) for the downflow. We note again that $\langle y_{TH} \rangle_n$ and $\langle y_{BC} \rangle_n$ are contributions, not compositions. As before, V_T represents the dead volume of top reservoir, and V_B the dead volume of the bottom. The symbol Q denotes the piston volume displaced.

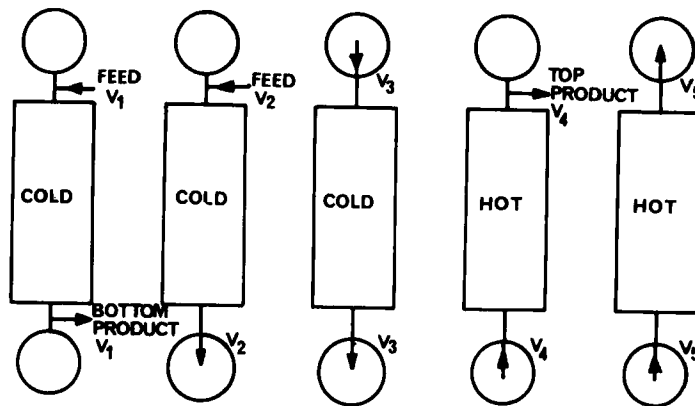


FIGURE 7a

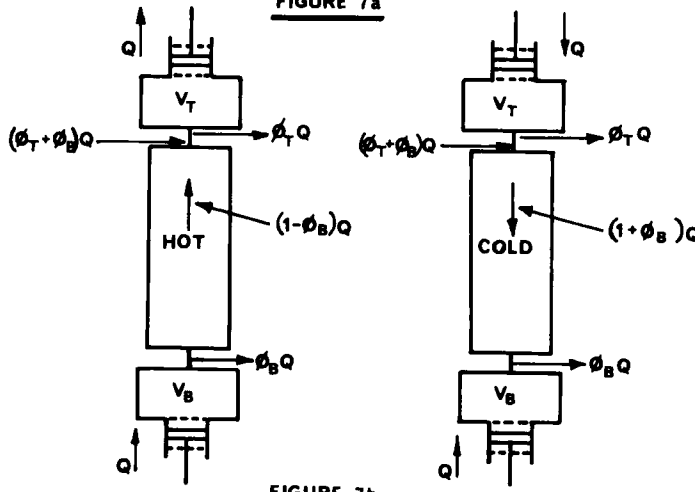


FIGURE 7b

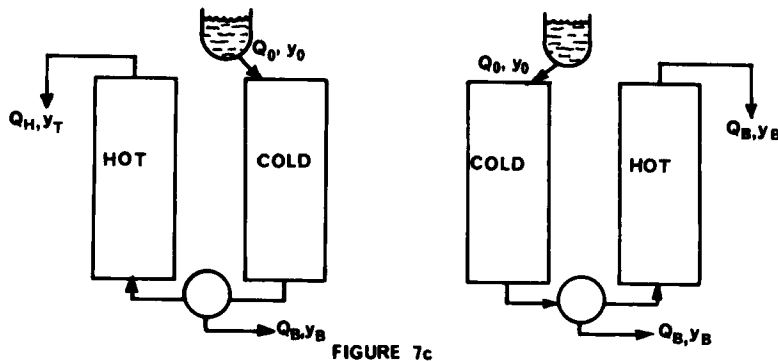


FIGURE 7c

Suggested types of continuous devices (a) After Chen and Hill⁽⁹⁾
 (b) After Gregory and Sweed⁽¹⁴⁾ (c) After Foo⁽⁴²⁾

External equations must be written to reflect the mass addition to and removal from the system. A schematic representation of how this was done in the Chen-Hill scheme is shown in Figure 7. In what follows, the subscript "H" refers to the hot upflow part of a cycle, while "C" denotes the cold downflow half-cycle. The fractions ϕ_T and ϕ_B refer to the fraction of the displacement volume Q removed at the top and bottom, respectively. The symbol $\langle y_{TPH} \rangle_n$ represents the top product composition which is removed from the system during the hot upflow part of the n^{th} cycle, while $\langle y_{TPC} \rangle_n$ represents the top product removed during cold downflow. At this point we comment on the symbolic method of operation outlined by Chen and Hill⁽⁹⁾. These workers show the feed entering just upstream to products withdrawal on upflow. This does not seem to be a sensible operating scheme, since feed is allowed to dilute the enriched stream leaving the top of the column. An alternate and perhaps better method of operation is suggested by Gregory and Sweed⁽¹⁴⁾. Their scheme is somewhat more complex, but appears to eliminate the dilution problem mentioned above. The U-tube scheme shown in Figure 7 can also be designed to minimize mixing of feed and enriched product.

Taking material balances around the feed point (Figure 7), gives for upflow:

$$(\phi_T + \phi_B)y_0 + (1-\phi_B)\langle y_{TH} \rangle_n = (1+\phi_T)\langle y_{TPH} \rangle_n \quad (86)$$

and downflow:

$$\begin{aligned} (\phi_T + \phi_B)y_0 + \langle y_{TPC} \rangle_n &= (\phi_T)\langle y_{TPC} \rangle_n \\ &+ (1+\phi_B)\langle y_{TC} \rangle_n. \end{aligned} \quad (87)$$

This can be written:

$$\langle y_{TPC} \rangle_n = \frac{1+\phi_B}{1-\phi_T} \langle y_{TC} \rangle_n - \frac{\phi_T + \phi_B}{1-\phi_T} y_0 \quad (88)$$

A solute balance on the top reservoir gives for upflow:

$$Q\pi/\omega \langle y_{TPH} \rangle_n + V_T \langle y_{TPC} \rangle_{n-1} \\ = (V_T + Q \frac{\pi}{\omega}) \langle y_{TPC} \rangle_n \quad (89)$$

which simply sums the amount of injected material plus the material contained in the reservoir before injection; the mixture of these gives the composition of material to be injected into the column during the following cold downflow half-cycle. It follows for the bottom section with continuous product withdrawal, the solute balance around the product removal point gives for downflow

$$\langle y_{BC} \rangle_n = \langle y_{BPC} \rangle_n \quad (90)$$

and for upflow

$$\langle y_{BH} \rangle_n = \langle y_{BPH} \rangle_n \quad (91)$$

To account for effects of dead volume in the bottom reservoir, a solute balance shows

$$Q \frac{\pi}{\omega} \langle y_{BC} \rangle_{n-1} + V_B \langle y_{BH} \rangle_{n-1} = (V_B + Q \frac{\pi}{\omega}) \langle y_{BH} \rangle_n \quad (92)$$

for similar reasons as following eq. (89).

Over the complete cycle, the average top product composition is simply

$$\langle y_{TP} \rangle_n = \frac{\langle y_{TPC} \rangle_n + \langle y_{TPH} \rangle_n}{2}$$

provided ϕ_T is the same for each half-cycle.

Since there are several dependent variables to choose for generating a finite-difference equation, we elect to eliminate the product composition variables and obtain an equation which can be solved in conjunction with the internal equations (eqs. 46 and 47). We first eliminate $\langle y_{TPH} \rangle_n$ by combining the top reservoir eq. (89) with the upflow feed-point balance, eq. (86), to give

$$\langle y_{TH} \rangle_n = \frac{1+\phi_T}{1-\phi_B} \left[\left(1 + \frac{V_T}{Q\pi/\omega} \right) \langle y_{TPC} \rangle_n \right. \\ \left. - \frac{V_T}{Q\pi/\omega} \langle y_{TPC} \rangle_{n-1} \right] - \frac{(\phi_T + \phi_B) y_0}{(1-\phi_B)} \quad (93)$$

Next, equation (88) is used to eliminate $\langle y_{TC} \rangle$, giving

$$\begin{aligned} \langle y_{TH} \rangle_n &= \frac{1+\phi_B}{T-\phi_T} \frac{1+\phi_T}{T-\phi_B} \left[\left(1 + \frac{V_T}{Q\pi/\omega} \right) \langle y_{TC} \rangle_n \right. \\ &\quad \left. - \frac{V_T}{Q\pi/\omega} \langle y_{TC} \rangle_{n-1} \right] - \frac{\phi_T + \phi_B}{T-\phi_B} \left[\frac{2}{T-\phi_T} \right] y_0 \end{aligned} \quad (94)$$

which is identical to the result of Chen and Hill⁽⁹⁾, except for a misprint in the second term, RHS.

We are now in a position to determine the relevant finite-difference relation by combining eqs. (46) and (47) with eq. (94); equating (46) and (34) gives

$$\begin{aligned} \frac{AB}{AD} \frac{1+b}{1-b} \langle y_{TC} \rangle_{n-1} &+ \frac{BC}{AD} \langle y_{BH} \rangle_{n-p-1} + \frac{CD}{AD} \langle y_{BH} \rangle_{n-p} \\ &= \frac{1+\phi_B}{T-\phi_T} \frac{1+\phi_T}{T-\phi_B} \left[\left(1 + \frac{V_T}{Q\pi/\omega} \right) \langle y_{TC} \rangle_n - \frac{V_T}{Q\pi/\omega} \langle y_{TC} \rangle_{n-1} \right] \\ &\quad - \frac{\phi_T + \phi_B}{T-\phi_B} \left[\frac{2}{T-\phi_T} \right] y_0 \end{aligned} \quad (95)$$

To determine the $\langle y_{BH} \rangle_n$ terms, we combine the bottom reservoir balance, eq. (92), with the internal balance, eq. (47), to give a first order finite-difference equation:

$$\frac{1-b}{1+b} \langle y_{BH} \rangle_{n-1} = \left(1 + \frac{V_B}{Q\pi/\omega} \right) \langle y_{BH} \rangle_n - \left(\frac{V_B}{Q\pi/\omega} \right) \langle y_{BH} \rangle_{n-1} \quad (96)$$

This has the solution assuming $\langle y_{BH} \rangle_n$ is y_0 at $n=1$,

$$\frac{\langle y_{BH} \rangle_n}{y_0} = \gamma^{n-1} \quad (97)$$

where the associated eigenvalue is:

$$\gamma = \frac{V_B/Q\pi/\omega + \left(\frac{1-b}{1+b} \right)}{1 + \frac{V_B}{Q\pi/\omega}} \quad (98)$$

The cold downflow composition, $\langle y_{BC} \rangle_n$, is obtained by inserting (97) into eq. (92), which gives

$$\langle y_{BC} \rangle_n = \left(\frac{1-b}{1+b} \right) \gamma^{n-1} = \langle y_{BPC} \rangle_n \quad (99)$$

These two important results represented by eqs. (97) and (99) agree with the underived results of Chen, Rak, Stokes and Hill⁽⁴⁴⁾.

The resulting eq. for $\langle y_{BH} \rangle_n$ is finally inserted into eq. (95), noting that the weighting factors from eq. (34) are calculated

using $L_C/L_H = \left(\frac{1+\phi_B}{1-\phi_B} \right) \left(\frac{1-b}{1+b} \right)$, since column displacement is not symmetric. When this is done, there results

$$\begin{aligned} \frac{L_C(1+b)}{L_H(1-b)} \langle y_{TC} \rangle_{n-1} + y_0(1 - L_C/L_H)[q \gamma^{n-p-2} + (1-q) \gamma^{n-p-1}] \\ = \langle y_{TC} \rangle_n \left[\frac{(1+\phi_B)(1+\phi_T)}{(1-\phi_B)(1-\phi_T)} \left(1 + \frac{V_T}{Q\pi/\omega} \right) \right] \\ - \langle y_{TC} \rangle_{n-1} \left[\frac{V_T}{Q\pi/\omega} \frac{1+\phi_B}{1-\phi_B} \frac{1+\phi_T}{1-\phi_T} \right] - 2y_0(\phi_T + \phi_B)/(1-\phi_B)(1-\phi_T) \end{aligned} \quad (100)$$

This is a tedious but simple finite-difference equation of the form $y_{n+1} - \lambda y_n = c + d^n$. The eigenvalue for the complementary solution is

$$\begin{aligned} \lambda = \left[\frac{V_T}{Q\pi/\omega} \frac{1+\phi_B}{1-\phi_B} \frac{1+\phi_T}{1-\phi_T} + \left(\frac{1+\phi_B}{1-\phi_B} \right) \right] \\ \cdot / \left[\frac{(1+\phi_B)}{(1-\phi_B)} \frac{(1+\phi_T)}{(1-\phi_T)} \left(1 + \frac{V_T}{Q\pi/\omega} \right) \right] \end{aligned} \quad (101)$$

and the general solution has the simple functional form

$$\langle y_{TC} \rangle_n = A\lambda^n + B\gamma^n + \langle y_{TC} \rangle_\infty$$

The technique to solve this problem proceeds exactly as the development for batch systems with dead volume given earlier. The solution was not completed by Chen and Hill in their first paper⁽⁹⁾ on the subject, but is given without derivation in a subsequent publication⁽⁴⁴⁾. The final results given⁽⁴⁴⁾ are not compact and are presented in such a tedious way as to obscure the simplicity of the findings, especially the dependence on the two underlying eigenvalues, γ and λ .

For $n < p+1$, the $\langle y_{BH} \rangle$ terms appearing on the LHS of eq. (95) are replaced with y_0 as before, giving

$$\frac{y_0}{K} \left(\frac{(1-L_c/L_H)}{(1-\phi_B)(1-\phi_T)} + \frac{2(\phi_B+\phi_T)}{(1-\phi_B)(1-\phi_T)} \right) = \langle y_{TC} \rangle_n - \lambda \langle y_{TC} \rangle_{n-1} \quad (102)$$

where

$$K = \frac{(1+\phi_B)(1+\phi_T)}{(1-\phi_T)(1-\phi_B)} \left(1 + \frac{V_T}{Q\pi/\omega} \right) \quad (103)$$

Similarly, the relationship for the case $n > p+1$, after rearranging eq. (99), is

$$\frac{y_0}{K} \left[\frac{2(\phi_B+\phi_T)}{(1-\phi_B)(1-\phi_T)} + (1-L_c/L_H)(q\gamma^{n-p-2} + (1-q)\gamma^{n-p-1}) \right] = \langle y_{TC} \rangle_n - \lambda \langle y_{TC} \rangle_{n-1} \quad (104)$$

Equations (102) and (104) comprise the system of finite-difference relations. The solution for $n < p+1$ is, taking $\langle y_{TC} \rangle_n = y_0$ at $n=1$:

$$\langle y_{TC} \rangle_n / y_0 = 1 + \frac{G}{1-\lambda} (1 - \lambda^{n-1}) \quad (105)$$

where

$$G = \left(\frac{(1-L_c/L_H)}{(1-\phi_B)(1-\phi_T)} + \frac{2(\phi_B+\phi_T)}{(1-\phi_B)(1-\phi_T)} \right) / K \quad (106)$$

The general solution to eq. (104) for $n > p+1$ is

$$\begin{aligned} \langle y_{TC} \rangle_n = A\lambda^n - \frac{(1-L_c/L_H)\lambda y_0}{K(1-\lambda)} (q\gamma^{n-p-2} + (1-q)\gamma^{n-p-1}) \\ + \frac{2(\phi_B+\phi_T)}{(1-\phi_B)(1-\phi_T)(1-\lambda)K} \end{aligned} \quad (107)$$

The arbitrary constant A is evaluated as before by coupling the two solutions at $n = p+1$, which gives

$$\begin{aligned} \frac{\langle y_{TC} \rangle_n}{y_0} = \lambda^{n-p-1} \left\{ 1 + \frac{(1-L_c/L_H)}{K(1-\lambda)} [(1-\lambda^p) + q\lambda/\gamma + (1-q)\lambda] \right. \\ \left. - \frac{2(\phi_B+\phi_T)}{K(1-\lambda)(1-\phi_B)(1-\phi_T)} \lambda^p \right\} \end{aligned}$$

$$\gamma^{n-p-1} \left\{ \frac{(1-L_c/L_H)\lambda y_0}{K(1-\lambda)} (q/\gamma + (1-q)) \right\} \\ + \left\{ \frac{2(\phi_B + \phi_T)}{(1-\phi_B)(1-\phi_T)(1-\lambda)} \right\} \quad (108)$$

The rate of enrichment is thus seen to be a simple function of the two system eigenvalue, γ and λ . Inspection of eq. (98) shows that for all cases $\gamma < 1$. Furthermore, for complete removal of solute we require $L_c \leq L_H < h$ giving $\frac{1+\phi_B}{1-\phi_B} \frac{1-b}{1+b} \leq 1$ which means $b \geq \phi_B$. Actually, complete solute removal is assured when $L_c < h$, which means $Q(1+\phi_B)\pi/\omega < h$, a useful relation for practical estimates. With this in mind, it is easy to see from eq. (101) that $\lambda < 1$, hence the ultimate concentration as $n \rightarrow \infty$ is

$$\frac{\langle y_{TC} \rangle_\infty}{y_0} = \frac{2(\phi_B + \phi_T)}{(1-\phi_B)(1-\phi_T)(1-\lambda)K} \quad (109)$$

which reduces to

$$\frac{\langle y_{TC} \rangle_\infty}{y_0} = \frac{\phi_B + \phi_T}{\phi_T(1+\phi_B)} \quad (110)$$

The top product composition at steady-state can be computed from this (or by a simple over-all balance) along with eq. (88) to give:

$$\frac{\langle y_{TPC} \rangle_\infty}{y_0} = \frac{\phi_B + \phi_T}{1-\phi_T} \left(\frac{1}{\phi_T} - 1 \right) = 1 + \phi_B/\phi_T \quad (111)$$

which is identical to the result of Chen and Hill⁽⁹⁾.

The theoretical results have been favorably compared with experiments using the system toluene - n-heptane on silica gel (44,45). The reader should bear in mind that $L_c \leq L_H < h$ for complete separation, hence $b \geq \phi_B$, where $\phi_B = B/Q$, (the ratio of bottom product volume to piston displacement volume).

Concluding Remarks

The equations for the equilibrium theory of batch and continuous systems have been derived and solved, including the im-

portant modifications to date, with special attention to a general solution technique. The solutions can be applied to semi-continuous operation when suitable modifications are applied.

For the first time, a simple asymptotic design relation for batch systems has been presented which includes the important dissipative effects associated with film resistance and axial mixing. The design relation gives ultimate steady-state separation, which is the maximum possible separation for the transient in a batch system. It has been shown that in the absence of dispersive forces, the new theory is in accord with the predictions of the equilibrium theory. Finally, it is demonstrated there exists an optimum frequency to maximize ultimate separation.

It is not expected that parametric pumping will become a traditional unit-operation, however there is now clear evidence in the literature that the technique constitutes an important option when conventional separation methods fail or become uneconomic.

It is suggested that a parapump-type process should be carefully considered as a candidate model for active human cell transport, with attention needed in uncovering the existence of a plausible retard-release mechanism.

Acknowledgements

This work was completed during the author's sabbatical leave at the University of Missouri-Columbia. The financial assistance and encouragement provided by Professor George Preckshot, Chairman of Chemical Engineering, is gratefully acknowledged.

Nomenclature

A = interstitial fluid displacement length
a = temperature coefficient, defined by eqn (17)
 a_h = particle area for heat transfer per unit particle volume
 a_p = particle area for mass transfer per unit particle volume
b = a/lm_0 , defined by eqn (19)
c = bulk fluid composition, moles/cc

c^*	= equilibrium fluid composition, moles/cc
c_f, c_s	= fluid, solid heat capacity, respectively
D	= diffusion coefficient
D_p	= pore diffusion coefficient
D_s	= diameter solid packing piece
E	= eddy dispersion coefficient
ΔH_{ads}	= heat of adsorption
h	= height of column (same as L)
h_p	= particle heat transfer coefficient
k_m	= mass transfer coefficient
k^*	= linear equilibrium constant, defined by eqn (68)
k_0, k_1	= equilibrium temperature coefficients, defined by eqn (68)
L	= length of packed column
L_c, L_H	= solute penetration lengths, defined by eqns (23) and (24)
M	= equilibrium constant, defined by eqn (9)
m	= equilibrium constant, defined by eqn (17)
m_0	= constant defined by eqn (17)
Pe_m	= Peclet number for mass transfer, $R^2 \omega / D$
p	= defined by eqn (33)
q	= defined by eqn (33) or used as solids composition as in eqn (4)
Q	= volumetric fluid displacement
r	= radial coordinate
R	= column radius
Re	= Reynolds number, $V_0 D_s / \nu$
Sc	= Schmidt number, ν / D
Sh	= Sherwood number, defined by eqn (69)
T	= fluid temperature
T_s	= solid packing temperature
t	= local time
V	= interstitial velocity
V_0	= superficial velocity
x	= solid composition, moles/gram solid
y	= fluid composition, moles/mole solvent
z	= axial coordinate

Greek

α	= thermal diffusivity
α_n	= separation factor for n^{th} cycle
α_b	= defined by eqn (67)
α_∞	= ultimate separation factor
β	= eigenvalue, defined by eqn (54)
Γ	= eigenvalue, defined by eqn (30)
γ	= eigenvalue, defined by eqn (98)
δ	= defined by eqn (66)
ϵ_b, ϵ_b	= pore and bulk voidages, respectively
λ	= eigenvalue, defined by eqn (101)
μ	= viscosity
ν	= kinematic viscosity
ρ_s, ρ_f	= solid, fluid densities, respectively
ϕ_B, ϕ_T	= bottom and top product volumes as fraction of Q
ω	= frequency

References

- (1) R. H. Wilhelm, A. W. Rice, and A. R. Bendelius, *Ind. Eng. Chem. Fundam.*, 5, 141 (1966).
- (2) R. H. Wilhelm and N. H. Sweed, *Science*, 159, 522 (1968).
- (3) R. H. Wilhelm, A. W. Rice, R. W. Rolke, and N. H. Sweed, *Ind. Eng. Chem. Fundam.*, 7, 337 (1968).
- (4) D. W. Thompson and D. Bass, *Can. Jour. Chem. Eng.*, 52, 345 (1974).
- (5) D. W. Thompson, D. Bass and M. E. Abu-goukh, *Can. Jour. Chem. Eng.*, 52, 479 (1974).
- (6) K. C. Lee and D. J. Kirwan, *Ind. Eng. Chem. Fundam.*, 14, 279 (1975).
- (7) P. C. Wankat, *Separ. Sci.*, 9, 85 (1974).
- (8) R. L. Pigford, B. Baker and D. E. Blum, *Ind. Eng. Chem. Fundam.*, 8, 144 (1969).
- (9) H. T. Chen and F. B. Hill, *Separ. Sci.*, 6, 411 (1971).

- (10) R. Aris, *Ind. Eng. Chem. Fundam.*, 8, 603 (1969).
- (11) D. W. Thompson and B. D. Bowen, *Ind. Eng. Chem. Fundam.*, 11, 417 (1972).
- (12) N. H. Sweed and R. H. Wilhelm, *Ind. Eng. Chem. Fundam.*, 8, 221 (1969).
- (13) R. G. Rice, *Ind. Eng. Chem. Fundam.*, 14, 362 (1975).
- (14) R. A. Gregory and N. H. Sweed, *Chem. Eng. Jour.*, 1, 207 (1970).
- (15) S. C. Foo and R. G. Rice, *AIChE Jour.*, 21, 1149 (1975).
- (16) H. K. Rhee and N. R. Amundson, *Ind. Eng. Chem. Fundam.*, 9, 303 (1970).
- (17) N. Wakao, H. Matsumoto, K. Suzuki, and A. Kawahara, *Kagaku Kogaku*, 32, 169 (1968).
- (18) Y. C. Hung and V. J. Lee, Paper 17c presented at 68th National Meeting of the AIChE, Houston (1971).
- (19) P. R. Harris, *Ind. Eng. Chem. Fundam.*, 9, 684 (1970).
- (20) R. A. Gregory, *AIChE Jour.*, 20, 294 (1974).
- (21) R. W. Rolke and R. H. Wilhelm, 8, 235 (1969).
- (22) R. G. Rice, *Ind. Eng. Chem. Fundam.*, 14, 202 (1975).
- (23) R. G. Rice, *Ind. Eng. Chem. Fundam.*, 13, 396 (1974).
- (24) R. G. Rice, *Ind. Eng. Chem. Fundam.*, 12, 406 (1973).
- (25) N. Wakao, T. Oshima, and S. Yagi, *Chem. Eng. Jap.*, 22, 780 (1958).
- (26) A. Klinkenberg and F. Sjenitzu, *Chem. Eng. Sci.*, 5, 258 (1956).
- (27) R. G. Rice and M. Mackenzie, *Ind. Eng. Chem. Fundam.*, 12, 486 (1973).
- (28) N. H. Sweed and R. A. Gregory, *AIChE Jour.*, 17, 171 (1971).
- (29) N. Hashimoto and J. M. Smith, *Ind. Eng. Chem. Fundam.*, 12, 353 (1973).
- (30) A. G. Shaffer and C. E. Hamrin, *AIChE Jour.*, 21, 782 (1975).
- (31) H. G. Schroeder and C. E. Hamrin, *AIChE Jour.*, 21, 807 (1975).
- (32) R. R. Patrick, J. T. Schrot, and R. I. Kermode, *Separ. Sci.*, 7, 331 (1972).

- (33) K. Weaver and C. E. Hamrin, *Chem. Eng. Sci.*, 29, 1873 (1974).
- (34) H. T. Chen, W. W. Lin, J. D. Stokes, and W. R. Fabisiak, *AIChE Jour.* 20, 306 (1974).
- (35) R. H. Wilhelm, "Intracellular Transport", *Symposia of the International Society for Cell Biology*, Vol. 5, p. 199, edited by K. B. Warren, Academic Press, New York (1966).
- (36) H. L. Booij, *Ind. Eng. Chem. Fundam.*, 8, 231 (1969).
- (37) R. G. Rice, *Ind. Eng. Chem. Fundam.*, 14, 280 (1975).
- (38) H. L. Booij, *Ind. Eng. Chem. Fundam.*, 14, 281 (1975).
- (39) Apostolopoulos, *Ind. Eng. Chem. Fundam.*, 14, 11 (1975).
- (40) F.J.M. Horn and C. H. Lin, *Ber. Bunsenges. Phys. Chem.*, 73, 575 (1969).
- (41) P. C. Wankat, *Ind. Eng. Chem. Fundam.*, 12, 372 (1973).
- (42) S. C. Foo, PhD Thesis, Univ. Queensland (Australia), (1976).
- (43) R. A. Gregory and N. H. Sweed, *Chem. Eng. Jour.*, 4, 139 (1972).
- (44) H. T. Chen, J. L. Rak, J. D. Stokes, and F. B. Hill, *AIChE Jour.*, 18, 356 (1972).
- (45) H. T. Chen, J. A. Park and J. L. Rak, *Separ. Sci.*, 9, 35 (1974).